THESIS APPROVED BY

4/22/2020

Date

Stephen M. Gross

Stephen M. Gross, Ph.D., Chair

Mark A. Latta

Mark A. Latta, D.M.D., M.S.

Barbara J. O'Kane

Barbara J. O'Kane, Ph.D., M.S.

Mark D, Markham

Mark. D. Markham, D.D.S

Gail M. Jensen, Ph.D., Dean

HANDLING CHARACTERISTICS AND COLLOIDAL STABILITY OF AN ORTHODONTIC SEALANT CONTAINING MICROCAPSULES

By

ALEXANDER BANKETOV

A THESIS

Submitted to the Faculty of the Graduate School of Creighton University in Partial Fulfillment of the Requirements for the Degree of Master of Science in the Department of Oral Biology

---

Omaha, NE

April 14, 2020

ABSTRACT

Patients treated with orthodontic brackets face an increased risk of biofilm accumulation which can lead to white spot lesions and ultimately cause cavitation. The application of an orthodontic sealant would act as a physical barrier between the bracket and superficial enamel. The sealant formulations contain microcapsules capable of releasing bioavailable remineralizing ions. The addition of the novel ion-releasing microcapsules within the sealant required the study of handling characteristics and colloidal stability of the formulations. Orthodontists require consistent and predictable handling which is reflected by colloidal stability. Multiple formulations were developed with varying ratios in the continuous phase, glass loading, and fumed silica loading to show their effect on flow and stability. Low stress monomers and a low viscosity monomer was utilized in the formulations. Results demonstrated that glass loading had an effect on flow and the low viscosity monomer had an effect on both flow and stability. The increase in glass loading decreased the average flow of formulations. The increase in low viscosity monomer ratio increased both flow rate and stability.

ACKNOWLEDGMENTS

I would like to thank Creighton University School of Dentistry and Dr. Neil Norton for providing me the opportunity to conduct research and contribute to the field of dentistry through this program. I would like to thank Dr. Stephen Gross for the countless hours spent within the classroom and lab mentoring me to become a better student and professional. Thank you to Dr. Mark Latta for providing the experience and resources that allowed this research to become possible. I would also like to thank Garret Hucal for all the hard work and effort put in the lab every day. Finally, I would like to thank Justin Pfeifer and Ben Kruse for greatly contributing to this research project. I am thankful for the experiences and relationships I have formed through this program.

TABLE OF CONTENTS

FIGURES AND TABLES

Chapter 1

Introduction

1.1 The Caries Process

Dental caries is known to be one of the most common infectious diseases throughout history. Nearly half of the global population suffers from untreated dental caries. Individuals are vulnerable to this disease throughout their entire lifetime. If not identified and treated by a dental professional early on, it can cause irreversible damage to dentition. Left untreated, the cavitation will progress through deeper tissues of the tooth ultimately leading to an abscess near the pulpal region of the tooth. This severe condition can lead to a bacterial infection and even death [1]. Individuals also risk gingivitis and periodontitis as untreated caries continues to progress. Specifically, primary dental caries damage the hard tissues of teeth through a process of acid erosion. These hard tissues include enamel, dentin, and cementum. The enamel is almost entirely made up of a natural mineral called hydroxyapatite [1,3]. It is a crystalline calcium phosphate structure. Dental caries is essentially a process of tooth demineralization [2].

Dental caries is caused by the acidic bacterial by-product from the consumption and fermentation of carbohydrates. Suitable tooth surface, acid producing bacteria, carbohydrates, and time are all required for dental caries to arise [3]. Even though there are thousands of different types of microbes that exist within the oral cavity, only a few cause dental caries. The two common bacteria associated with caries are *Streptococcus mutans* and *Lactobacillus* [1,2]. The caries process begins with biofilm, dental plaque, covering a suitable tooth environment. These preferred environments include the pits, fissures, and facial sides of teeth. Dental biofilm begins as an adhesive, colorless bacterial mass and becomes more yellow as the growth continues. The biofilm's other main components are characterized as mostly inorganic and organic materials such as sugars and glycoproteins [1].

If dental plaque isn't removed from the surface of the tooth, it continues to develop and thicken around the enamel. As this biofilm grows, the amount of oxygen decreases making the environment favorable for anaerobic bacteria. The further consumption of carbohydrates creates lactic acid as a byproduct. This acid decreases the pH of the oral environment and further establishes a favorable surrounding for caries-causing microbes such as *Streptococcus mutans* and *Lactobacillus.* The increased consumption of sugars by the microbes in the acidic environment continues to decrease the pH. Once the pH drops below 5.5, the demineralization process begins. This point is known as the critical pH of enamel, or hydroxyapatite (HAP). HAP is primarily composed of calcium, phosphate, and hydroxyl ions ($Ca_{10}(PO_4)_6(OH)_2$). Critical pH is the point where a solution is saturated with a particular mineral. In this case, it's tooth enamel with calcium and phosphate ions. Saliva contains calcium, phosphate, and bicarbonate ions which act as a buffer system to help neutralize the pH of the environment. There is a dynamic equilibrium of precipitation and dissolution that exists between the superficial enamel and surrounding oral fluids. If the solution pH is above the critical pH, it's supersaturated with calcium and phosphate minerals which, as a result, will precipitate and remineralize the enamel surface. If the solution pH is below the critical pH, it's unsaturated and will lead to the dissolution of enamel into its respective ions until saturation [16,17,21].

Hydroxyapatite is a highly insoluble mineral. The K_{sp} of HAP is 10^{-59}. K_{sp} is the solubility product constant which expresses the degree to which a compound dissociates in a solution. Lower K_{sp} indicates a lower degree of solubility. When fluoride is introduced, it has the potential to replace the hydroxyl ions in the apatite structure. This reaction produces fluorapatite, $Ca_{10}(PO_4)_6F_2$, (FAP) which has a K_{sp} of 10^{-60}, making it less soluble than HAP. This means that FAP is harder to demineralize than HAP. FAP has a critical pH of 4.5, which is lower than that of

HAP which is 5.5. Fluoride acts to create a more acid-resistant structure due to its lower critical pH and lower solubility relative to tooth structure. It also interferes with pellicle and plaque formation, suppressing microbial growth [16,17,21].

The tooth first begins to appear white as an initial sign of demineralization. This is also known as a white spot lesion. As time progresses, the area of cavitation becomes darker to shades of brown or black when major demineralization has occurred [3]. This all happens over a period of time and there is an opportunity for remineralization to occur before irreversible damage is caused by cavitation. Through mechanical cleaning, remineralization by saliva, and the addition of fluoride ions from an outside source, the pH can be raised to a normal level and the caries process is halted [2].

1.2 Orthodontic Brackets and Demineralization

Patients treated with orthodontic brackets are at a higher risk for greater biofilm growth and white spot lesion formation [3]. This is an area of decalcification and is the major precursor to the development of dental caries. Due to the nature of a fixed bracket, good oral hygiene is necessary to prevent plaque build up and ultimately demineralization [4]. An orthodontic bracket creates more difficult to reach places for mechanical cleaning methods. The average age of an orthodontic bracket patient is between 10 - 14 years. Noncompliance with increased oral hygiene has negative effects with dental plaque accumulation. If the patient's diet contains high quantities of acidic foods or drinks, dental biofilm growth rate is increased. In addition to the potential damage to dentition, the increase of financial cost and adjusted length of orthodontic treatment is another burden for the patient [5,6]

Enamel experiencing demineralization requires the uptake of available fluoride ions to remineralize the apatite and return to a healthy state. Most external sources of bioavailable fluoride ions, such as water and oral hygiene products, are only present on the enamel for short periods of time. Enamel facing a cariogenic challenge requires even more fluoride and these sources aren't enough to cover the deficit. The use of calcium can create a fluoride reserve in the form of CaF_2. Once formed on the enamel, CaF_2 is able to release fluoride ions for a longer period of time onto the enamel allowing a reaction to produce a less soluble fluorapatite. This becomes especially important during orthodontic treatment due to the ease and tendency of white spot lesion formation. The addition of calcium ions in the orthodontic sealant will allow this formation of CaF_2 to act as a fluoride reservoir [18].

1.3 Orthodontic Sealants and Microcapsules

During orthodontic treatment using brackets, enamel demineralization has been a common and recurring problem. To counteract this complication, the use of an orthodontic sealant could help prevent the accumulation of dental plaque. An orthodontic sealant is applied to the tooth before the bracket is placed. It acts as a physical barrier and protective measurement around the placed bracket. The microcapsules located within the sealant release remineralizing ions as locations around the bracket are favorable for plaque buildup preceding a cariogenic challenge. Pro Seal® and Opal® Seal™ are two orthodontic sealants that exist on the market today. They are resin-based fluoride releasing sealants that contain bioactive glass technology. These bioactive glasses interact with body fluids to release remineralizing ions such as fluoride, calcium, and phosphate. In addition, they are used as physical barriers and interfere with bacterial adherence with the main goal of protecting the superficial enamel from acid penetration.

A recent study reported the release of fluoride ions from Pro Seal® and Opal® Seal™, pertaining to the prevention of white spot lesions. In this study, fluoride release from bioactive glasses found within the sealant was observed for a period of 28 days. The bioactive glass was found to release most of its ion reservoir within a few days. It was noticed the release of fluoride from the sealants would help remineralize surface enamel. However, according to the study, "...it would not likely aid in the prevention of demineralization as there is no prolonged duration of fluoride release" [19].

An alternative to bioactive glasses that addresses the issue of short-term ion release has been reported recently. This study shows the potential of using microcapsules in sealants in order to prolong and create the gradual, controlled release of bioavailable ions to cover the entire duration of orthodontic treatment. The average orthodontic treatment generally lasts for a duration of 18 months [19]. The microcapsules are composed of an ion permeable polyurethane membrane and contain hypertonic aqueous solutions of either calcium, phosphate, or fluoride containing salts. Unlike the bioactive glasses which release their entire ion reservoir in a quick burst, the microcapsules serve as an ion permeable barrier that allows for long term, sustained release of remineralizing ions. This is due to the fact that it is diffusion controlled and driven by differences in concentration gradients found between the encapsulated aqueous solution contained within the microcapsules and the environment in which they are embedded. While fluoride has been used solely in some remineralization therapy and caries prevention products, the advantage of incorporating calcium and phosphate ions is considered to be beneficial. This is due to saliva containing all three previously mentioned ions which help prevent the breakdown of hydroxyapatite and it would promote the formation of CaF_2, a source of longer-term fluoride release [7].

A related previous study observed the overall effectiveness utilizing microcapsules in pit and fissure sealants. One part of the study compared a sealant with microcapsules containing an aqueous solution of remineralizing ions (calcium, phosphate, and fluoride) to a control sealant without microcapsules. It was found that incorporating microencapsulated remineralizing ions promoted fluoride uptake into demineralized enamel as compared to the control sealant without microcapsules. Additionally, it was found that the incorporation of calcium containing microcapsules increased the amount of enamel fluoride uptake relative to a fluoride only releasing sealant [20].

1.4 Utilization of Low Stress Monomers

Secondary caries, or recurrent caries, are largely influenced by volumetric shrinkage of dental resin composites. This is a type of dental composite failure. It's a natural occurrence during the polymerization of composites and one could typically expect 1.5-5% of volumetric shrinkage [14]. Volumetric shrinkage is the reduction of volume due to the increase in density [8]. Before polymerization has occurred, the monomers are at a Van der Waals radii from one another. Once the degree of conversion has increased (formation of the polymer), covalent bonds are established and the distance has decreased. The shrinkage leads to the development of internal stress [9,10]. Consequently, this all could lead to microfractures in the tooth structure and/or composite failure. The volumetric shrinkage could also lead to failure at the adhesive layer between the composite and the tooth structure. The new space formed by this creates a preferred area for dental plaque accumulation and the beginning of a recurring secondary caries [3,8]. This implementation of low stress monomers will improve mechanical properties by relieving internal stress and minimizing microfractures. They will reduce the spaces created at margins which lead to leakage.

There have been previous attempts in different studies to minimize the volumetric shrinkage. The two most effective ways are through manipulating the formulation with the addition of fillers or adjusting the curing method [13]. The addition of a filler such as silica, quartz, or mica, have been found to reduce internal stress production. Passive fillers such as polystyrene beads or polyvinyl chloride powder could also be added with similar effects on reducing volumetric shrinking [14,8]. The use of high molecular weight monomers have been found to be slightly effective as their benefits are limited due to increased viscosity resulting in poor handling characteristics. The practice of incremental filling as opposed to bulk fill method has been used to help reduce stress. Low-viscosity flowable composites have also been implemented to absorb some shrinkage stress. With the curing method, a pulse-delay technique can be utilized [13]. This is where a lower energy pulse is used initially with a brief intermission then continue with a higher energy pulse to finish curing the composite. The short break in between curing times helps relieve the strain within the composite before the final cure [12,8].

1.5 Handling Characteristics and Colloidal Stability

Viscosity is one of the most important attributes when discussing the handling characteristics of a dental composite. Typically, an orthodontist might require a higher viscosity formulation for placement of orthodontic brackets, whereas a general dentist might require a composite with a lower viscosity for the placement of a sealant. Packable composite mixtures are more highly filled with particles giving them a more viscous flow. They are preferred for larger fills and especially for posterior restorations. Flowable resin composites are less filled in order to achieve lower viscosity. They are used to easily cover all necessary surfaces during a restoration procedure. It helps create a better seal between the tooth and the composite as it’s more able to fill

microfractures and other structural defects. Flowable composites also reduce overall volumetric shrinkage as it's able to better absorb the internal stress [15]. Due to oral health professionals requiring products with a range of viscosities for certain procedures, manufacturers have produced composites with a range of flow properties. Along with viscosity, other important characteristics include stickiness, resistance to slumping after modeling, and yield point. [14].

Ideally, an individual applying an orthodontic sealant would require a low enough viscosity in order to cover the entire tooth surface. However, the viscosity must also be high enough to not run past the margins of the tooth. Colloidal stability is essential for predictable and consistent handling characteristics such as yield point and post shear stress flow. Yield point is the resistance to the initial flow of a fluid. The addition of fumed silica, a type of nanofiller, will serve to stabilize the colloid by preventing phase separation between the continuous phase and the filler phase. The continuous phase consists of liquid monomers and the filler phase consists of glass particles. Once mixed together, the acrylate monomers and glass particles are not soluble and tend to phase separate creating visible colloidal instability. Fumed silica will establish stabilization through electrostatic repulsion in order to provide consistent handling characteristics for an orthodontist.

In our study, handling characteristics and colloidal stability will be observed with a new type of orthodontic sealant that includes the novel ion-releasing microcapsules. The introduction of remineralizing microcapsules within the new orthodontic sealant requires the examination of handling characteristics and colloidal stability. Therefore, we created multiple formulations that varied by continuous phase, glass loading, and fumed silica loading to show their effect on flow and stability.

Chapter 2

Methods

2.1 Prepolymer Synthesis

A polyurethane prepolymer was synthesized by a solution polymerization in cyclohexanone (Sigma Aldrich). Polyurethane was synthesized using isophorone-diisocyanate (Fluka) and ethylene glycol (Sigma Aldrich). First, a flask was evacuated and flame-dried. Afterwards, nitrogen gas was slowly introduced to the flask. Cyclohexanone was then added while nitrogen gas continued to flow through the flow adapter. Using a syringe, the isophorone-diisocyanate was added. The septum was replaced and secured. A syringe needle was inserted through the septum, to relieve pressure inside the flask, while the solution stirred for 30 minutes. Then, ethylene glycol and an initiator were added. The septum was replaced a final time and secured. Next, the flask was lowered into an oil bath. A degassing needle, connected to the manifold, was inserted until it rested at the bottom of the flask. Then the adjacent inert gas port on the manifold (connecting to the hose of the degassing needle) was opened slowly until the reaction mixture began to bubble. Once complete, the solution degassed at room temperature for 30 minutes. After, the degassing needle was removed and the reaction mixture was set to 70°C. Once the temperature was set, the reaction ran overnight.

After overnight, the flask was removed from the oil bath and cooled for one hour. The solution was transferred, fitted to a flow adapter, and secured to a vacuum line from a cold trap. The dewar was filled approximately one third of the way with isopropanol (Fisher Scientific). Dry ice was added to the dewar in small pieces while the cold trap was in place. Once complete, the round bottom flask was lowered into the oil bath, and set to 100°C. All exposed glassware including the cold trap, flow adapter, and round bottom flask were insulated.

The flask was then evacuated, so that the evaporating solvent could travel into the trap and liquefy in a cold environment. The vacuum was pulled until the prepolymer appeared dry and all

solvent was recovered from the product. The pre-polymer was then collected and stored in vials in a cabinet at room temperature until microcapsule synthesis.

2.2 Preparation of Oil Solution and Salt Solution

The oil solution consisted of methyl benzoate (Acros), an emulsifying agent, and the polyurethane prepolymer. The three components were combined in an Erlenmeyer flask and stirred until the polyurethane was dispersed. It is important to note that the oil solutions were made at least 24 hours prior to microcapsule synthesis.

The salt solutions were made at various molarities desired for ion release. For this experiment, we made 3.0 M potassium phosphate dibasic (Fisher Scientific, New Jersey), 5.0 M calcium nitrate tetrahydrate (Alfa Aesar, Massachusetts) and 0.8 M sodium fluoride (MP Biomedicals, Ohio). It is important to note that higher concentrations of salts were added slowly in some cases over a period of a few days to dissolve. Solutions were stored at room temperature.

2.3 Microcapsule Synthesis

A reverse emulsion forms when the prepolymer oil solution is agitated at 70°C and the aqueous salt solution was gradually added. The polyurethane was then chain extended using ethylene glycol or diethylene glycol to finish preparing the microcapsules. The microcapsules were then transferred to centrifuge tubes and centrifuged in a Fisher Centrific 288 (Fisher Scientific, New Jersey).

2.4 Orthodontic Sealant Formulations

Urethane dimethacrylate (UDMA), Triethylene glycol dimethacrylate (TEGMA), low stress monomers (Terathane 1000 methacrylate and terathane 650 acrylate), a low viscosity monomer [hydroxypropyl methacrylate (HPM)], were the monomers used as the continuous phase in the orthodontic sealant formulations. The formulation ratio consisted of varying w/w% loadings of UDMA, TEGMA, low stress monomers (Terathane 1000 methacrylate and terathane 650 acrylate) (DM Healthcare Products, Inc), and low viscosity monomer (HPM). The photoinitiators used were then added 0.2 w/w% of camphorquinone and ethyl-4- dimethylaminobenzoate 7 w/w% of microcapsules including 0.8 M sodium fluoride, 5.0 M calcium nitrate tetrahydrate, 3.0 M potassium phosphate dibasic salt solutions, and different amounts of Schott glass and Evonik fumed silica. Tables 1-10 report all of the formulations that were prepared to analyze handling characteristics via flow tests.

Continuous Phase Ratio (UDMA/TEGMA/LVM/LSM)	Glass (w/w%)	FS (w/w%)	Low Stress Monomer
40/40/0/20	38	2.00	1000 Meth
30/40/10/20	38	2.00	1000 Meth
25/40/15/20	38	2.00	1000 Meth
20/40/20/20	38	2.00	1000 Meth
15/40/25/20	38	2.00	1000 Meth

Table 1. Formulations of orthodontic sealants containing 1000 Meth in the continuous phase. UDMA and LVM are varied while glass loading, fumed silica, TEGMA, and LSM are held constant.

Continuous Phase Ratio (UDMA/TEGMA/LVM/LSM)	Glass (w/w%)	FS (w/w%)	Low Stress Monomer
40/40/0/20	38	2.00	650 ACR
30/40/10/20	38	2.00	650 ACR
25/40/15/20	38	2.00	650 ACR
20/40/20/20	38	2.00	650 ACR
15/40/25/20	38	2.00	650 ACR

Table 2. Formulations of orthodontic sealants containing 650 ACR in the continuous phase. UDMA and LVM are varied while glass loading, fumed silica, TEGMA, and LSM are held constant.

Continuous Phase Ratio (UDMA/TEGMA/LVM/LSM)	Glass (w/w%)	FS (w/w%)	Low Stress Monomer
30/35/15/20	38	2.00	1000 Meth
30/30/20/20	38	2.00	1000 Meth
30/25/25/20	38	2.00	1000 Meth
30/20/30/20	38	2.00	1000 Meth

Table 3. Formulations of orthodontic sealants containing 1000 Meth in the continuous phase. TEGMA and LVM are varied while glass loading, fumed silica, UDMA, and LSM are held constant.

Continuous Phase Ratio (UDMA/TEGMA/LVM/LSM)	Glass (w/w%)	FS (w/w%)	Low Stress Monomer
40/40/0/20	50	2.00	1000 Meth
30/40/10/20	50	2.00	1000 Meth
25/40/15/20	50	2.00	1000 Meth
20/40/20/20	50	2.00	1000 Meth
15/40/25/20	50	2.00	1000 Meth

Table 4. Formulations of orthodontic sealants containing 1000 Meth in the continuous phase. UDMA and LVM are varied while glass loading, fumed silica, TEGMA, and LSM are held constant.

Continuous Phase Ratio (UDMA/TEGMA/LVM/LSM)	Glass (w/w%)	FS (w/w%)	Low Stress Monomer
40/40/0/20	45	2.00	1000 Meth
30/40/10/20	45	2.00	1000 Meth
25/40/15/20	45	2.00	1000 Meth
20/40/20/20	45	2.00	1000 Meth
15/40/25/20	45	2.00	1000 Meth

Table 5. Formulations of orthodontic sealants containing 1000 Meth in the continuous phase. UDMA and LVM are varied while glass loading, fumed silica, TEGMA, and LSM are held constant.

Continuous Phase Ratio (UDMA/TEGMA/LVM/LSM)	Glass (w/w%)	FS (w/w%)	Low Stress Monomer
40/40/0/20	45	2.00	650 ACR
30/40/10/20	45	2.00	650 ACR
25/40/15/20	45	2.00	650 ACR
20/40/20/20	45	2.00	650 ACR
15/40/25/20	45	2.00	650 ACR

Table 6. Formulations of orthodontic sealants containing 650 ACR in the continuous phase. UDMA and LVM are varied while glass loading, fumed silica, TEGMA, and LSM are held constant.

Continuous Phase Ratio (UDMA/TEGMA/LVM/LSM)	Glass (w/w%)	FS (w/w%)	Low Stress Monomer
40/40/0/20	50	2.00	650 ACR
30/40/10/20	50	2.00	650 ACR
25/40/15/20	50	2.00	650 ACR
20/40/20/20	50	2.00	650 ACR
15/40/25/20	50	2.00	650 ACR

Table 7. Formulations of orthodontic sealants containing 650 ACR in the continuous phase. UDMA and LVM are varied while glass loading, fumed silica, TEGMA, and LSM are held constant.

Continuous Phase Ratio (UDMA/TEGMA/LVM/LSM)	Glass (w/w%)	FS (w/w%)	Low Stress Monomer
30/35/15/20	45	2.00	650 ACR
30/30/20/20	45	2.00	650 ACR
30/25/25/20	45	2.00	650 ACR
30/20/30/20	45	2.00	650 ACR

Table 8. Formulations of orthodontic sealants containing 650 ACR in the continuous phase. TEGMA and LVM are varied while glass loading, fumed silica, UDMA, and LSM are held constant.

Continuous Phase Ratio (UDMA/TEGMA/LVM/LSM)	Glass (w/w%)	FS (w/w%)	Low Stress Monomer
35/30/15/20	38	2.00	650 ACR
30/30/20/20	38	2.00	650 ACR
25/30/25/20	38	2.00	650 ACR
20/30/30/20	38	2.00	650 ACR

Table 9. Formulations of orthodontic sealants containing 650 ACR in the continuous phase. UDMA and LVM are varied while glass loading, fumed silica, TEGMA, and LSM are held constant.

Continuous Phase Ratio (UDMA/TEGMA/LVM/LSM)	Glass (w/w%)	FS (w/w%)	Low Stress Monomer
20/40/20/20	38	1.50	650 ACR
20/40/20/20	38	1.75	650 ACR
20/40/20/20	38	2	650 ACR
20/40/20/20	38	2.25	650 ACR
20/40/20/20	38	2.50	650 ACR

Table 10. Formulations of orthodontic sealants containing 650 ACR in the continuous phase. Fumed silica is varied while glass loading, UDMA/TEGMA, LSM, and LVM are held constant.

2.5 Handling Characteristics and Colloidal Stability Test

To understand the handling characteristics and colloidal stability of the formulations, the flow distance of each formulation was measured as a function of time. A relatively constant post shear flow was used to indicate colloidal stability. In the experiment, 0.15g of the formulation was placed on to a microscope glass slide. The glass slide was placed vertically at 90 degrees and the formulation was allowed to flow for 60 seconds. The flow distance of the composite was marked on the slide at 30 seconds and 60 seconds. The flow distance was measured using a caliper. The flow distance test was tested for each formula initially followed by 72 hours and periodically for a 3-month period. As a reference point, the flow distance of Opal Seal was measured. Opal Seal had a flow distance of approximately 6 mm after 30 seconds and 9 mm after 60 seconds by the same test method.

Chapter 3

Results

3.1 Constant Low Stress Monomer

The effect of constant low stress monomers, glass loading, and fumed silica loading on flow with varying amounts of UDMA or TEGMA and low viscosity monomer (HPM) used in the continuous phase as a function of time was determined. Figures 1-9 report the flow of the various formulations with a constant monomer and glass loading over a 90-day period.

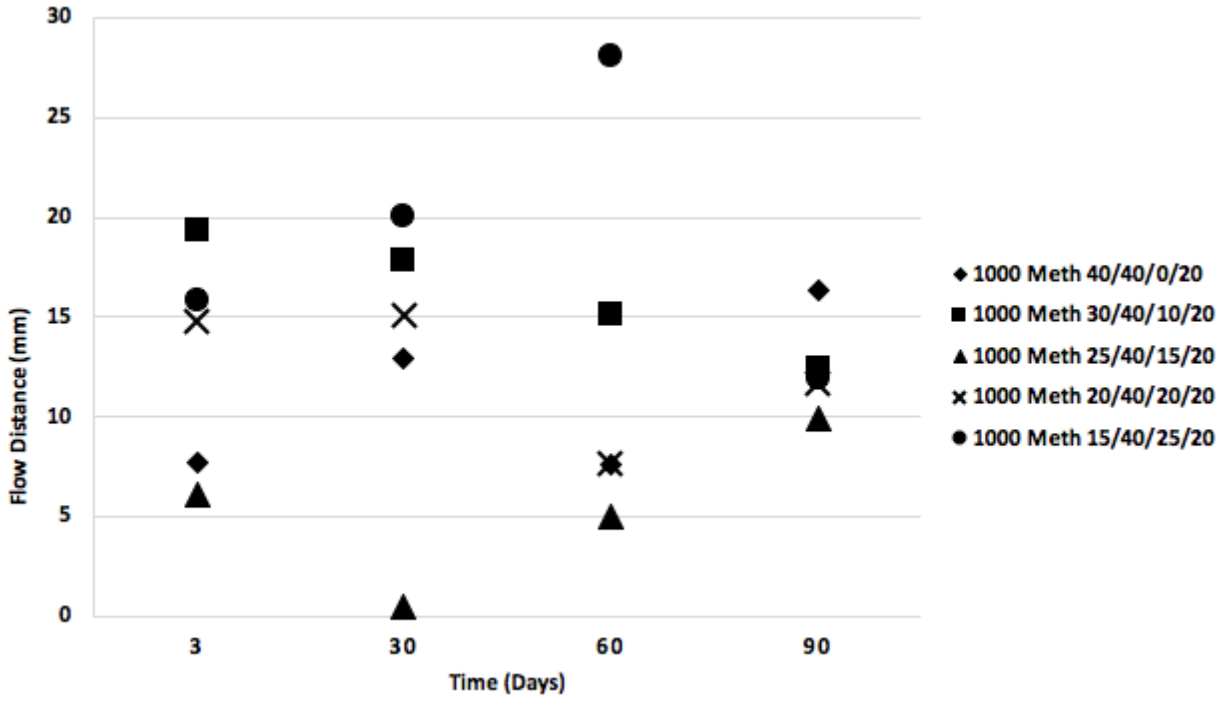

Figure 1. This graph illustrates the distance a constant mass of 1000 Meth formulation flowed in 30 seconds as a function of time after the formulation was prepared. The 5 different formulation identities differ by continuous phase ratio of UDMA and LVM presented as UDMA/TEGMA/LVM/LSM. Each formulation was loaded with 38 w/w% glass, 2 w/w% fumed silica, and 7 w/w% microcapsules.

Figure 1 depicts the flow of five different 1000 meth formulations in the ratios presented as UDMA/TEGMA/LVM/LSM with a constant low stress monomer and TEGMA ratio with a varying UDMA and LVM (HPM) ratio. Each formulation was loaded with 38 w/w% glass, 2 w/w% fumed silica, and 7 w/w% microcapsules. 30/40/10/20 reported to have the largest initial

flow on day three at 19.4 mm. The largest flow throughout the entire 90-day period was seen on day 60 by 15/40/25/20 at 28.1 mm. The formulation 25/40/15/20 was recorded having a flow of 0.5 mm on day 30 with an initial flow of 6.1 mm.

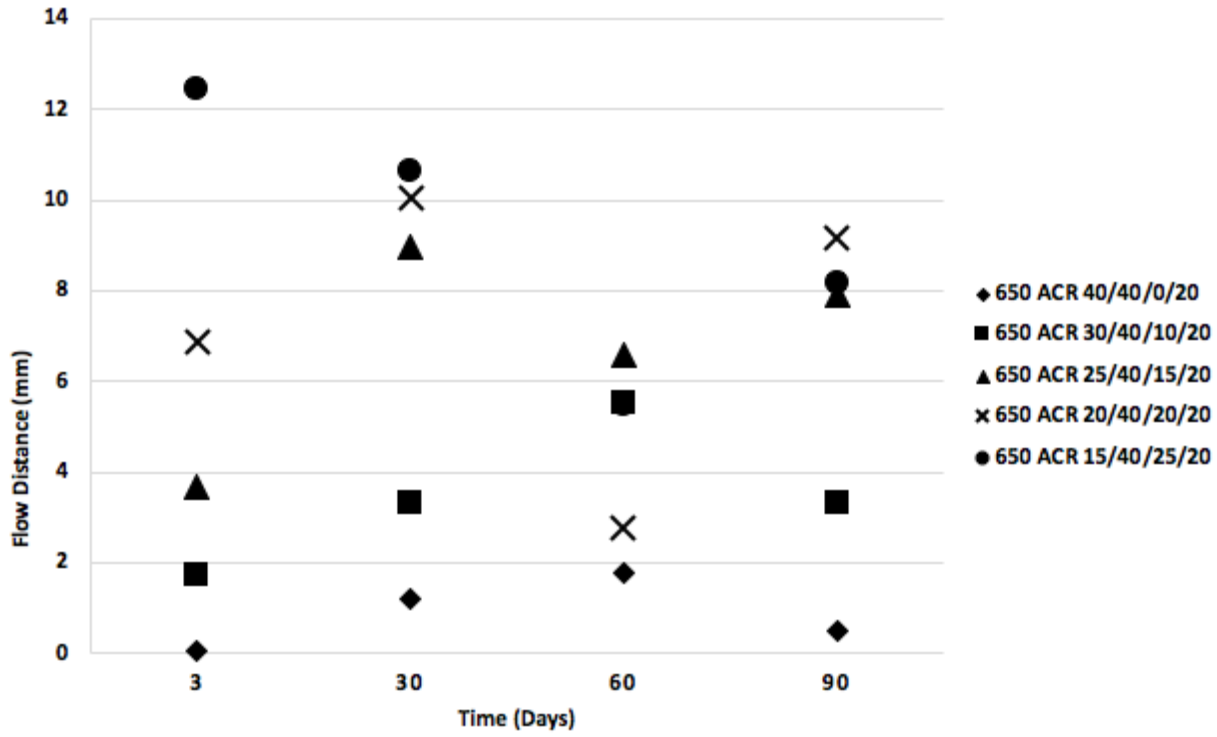

Figure 2. This graph illustrates the distance a constant mass of 650 ACR formulation flowed in 30 seconds as a function of time after the formulation was prepared. The 5 different formulation identities differ by continuous phase ratio of UDMA and LVM presented as UDMA/TEGMA/LVM/LSM. Each formulation was loaded with 38 w/w% glass, 2 w/w% fumed silica, and 7 w/w% microcapsules.

Figure 2 differs from figure 1 by changing the low stress monomer to 650 ACR. All of the formulations have the same continuous phase ratio as compared to figure 1. Within the continuous phase, UDMA and LVM are varied while all else is held constant. Each formulation was loaded with 38 w/w% glass, 2 w/w% fumed silica, and 7 w/w% microcapsules. The largest initial and overall flow within the 90-day period was recorded by 15/40/25/20 at 12.4 mm. The lowest initial flow was 0.06 mm by 40/40/0/20.

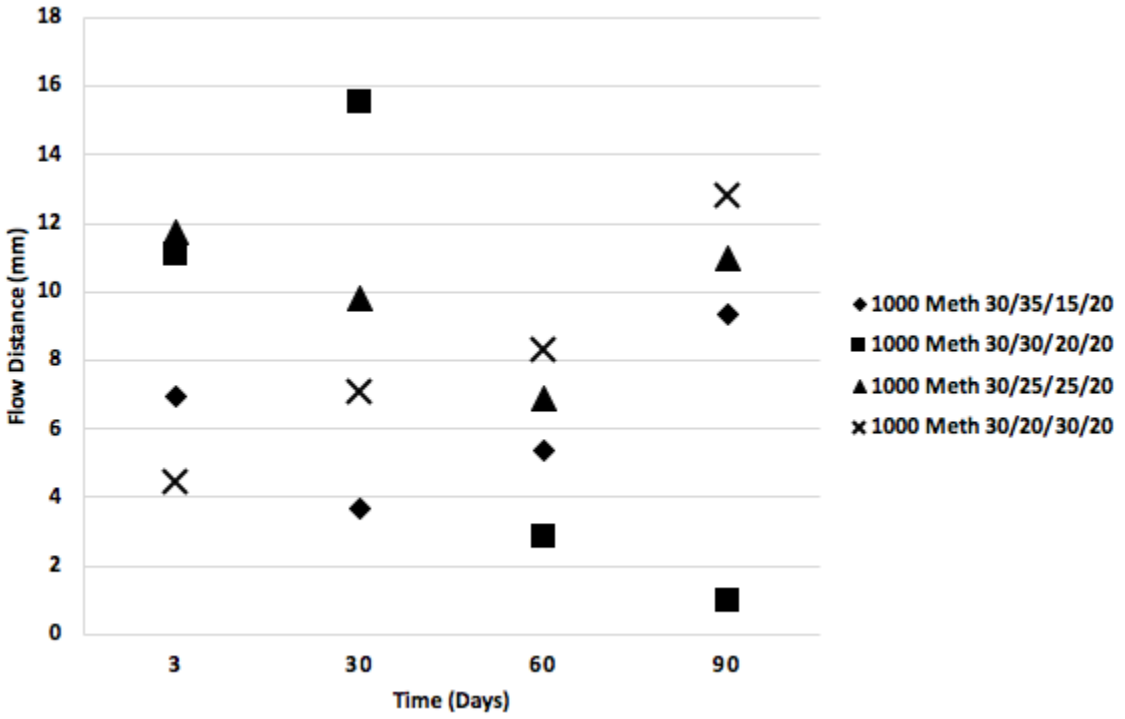

Figure 3. This graph illustrates the distance a constant mass of 1000 Meth formulation flowed in 30 seconds as a function of time after the formulation was prepared. The 5 different formulation identities differ by continuous phase ratio of TEGMA and LVM presented as UDMA/TEGMA/LVM/LSM. Each formulation was loaded with 38 w/w% glass, 2 w/w% fumed silica, and 7 w/w% microcapsules.

Figure 3 differs from the previous figures by different continuous phase ratios. The 4 different formulations contain 1000 Meth as the low stress monomer. TEGMA and LVM are varied in the continuous phase ratio. Each formulation within the set contained 38 w/w% glass loading, 2 w/w% fumed silica loading, and 7 w/w% microcapsules. The largest initial flow was recorded to be 11.7 mm by 30/25/25/20. The lowest initial flow was 4.5 mm by 30/20/30/20. The largest flow was 15.6 mm on day 30 by 30/30/20/20. The smallest flow distance was 1.0 mm on day 90 also by 30/30/20/20.

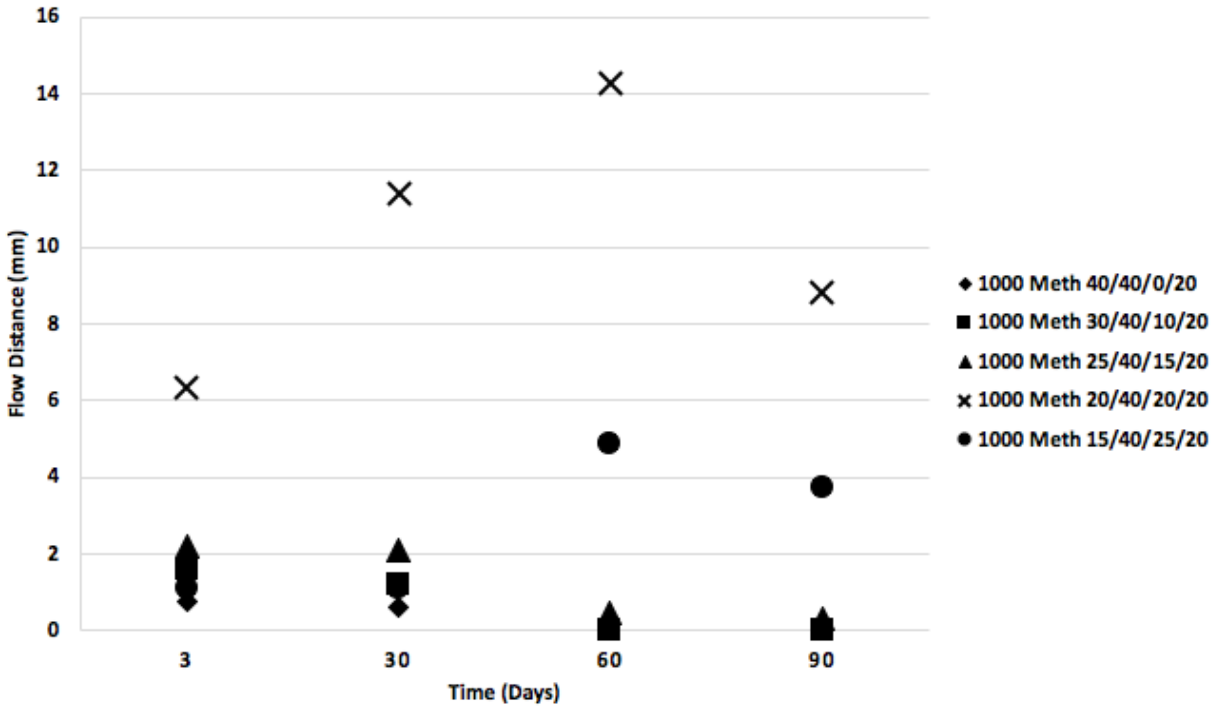

Figure 4. This graph illustrates the distance a constant mass of 1000 Meth formulation flowed in 30 seconds as a function of time after the formulation was prepared. The 5 different formulation identities differ by continuous phase ratio of UDMA and LVM presented as UDMA/TEGMA/LVM/LSM. Each formulation was loaded with 50 w/w% glass, 2 w/w% fumed silica, and 7 w/w% microcapsules.

Figure 4 differs from figures 1 and 2 by changing the glass loading to 50 w/w% from 38 w/w%. The 5 different formulation identities all contained 1000 Meth as the low stress monomer. Each formulation contained 50 w/w% glass loading, 2 w/w% fumed silica loading, and 7 w/w% microcapsules. The formulations differed by continuous phase ratio of UDMA and LVM. The largest initial flow was 6.4 mm by 20/40/20/20. The smallest flow distance was 0.8 mm by 40/40/0/20. The largest overall flow distance throughout the entire 90-day period was 14.3 mm by 20/40/20/20.

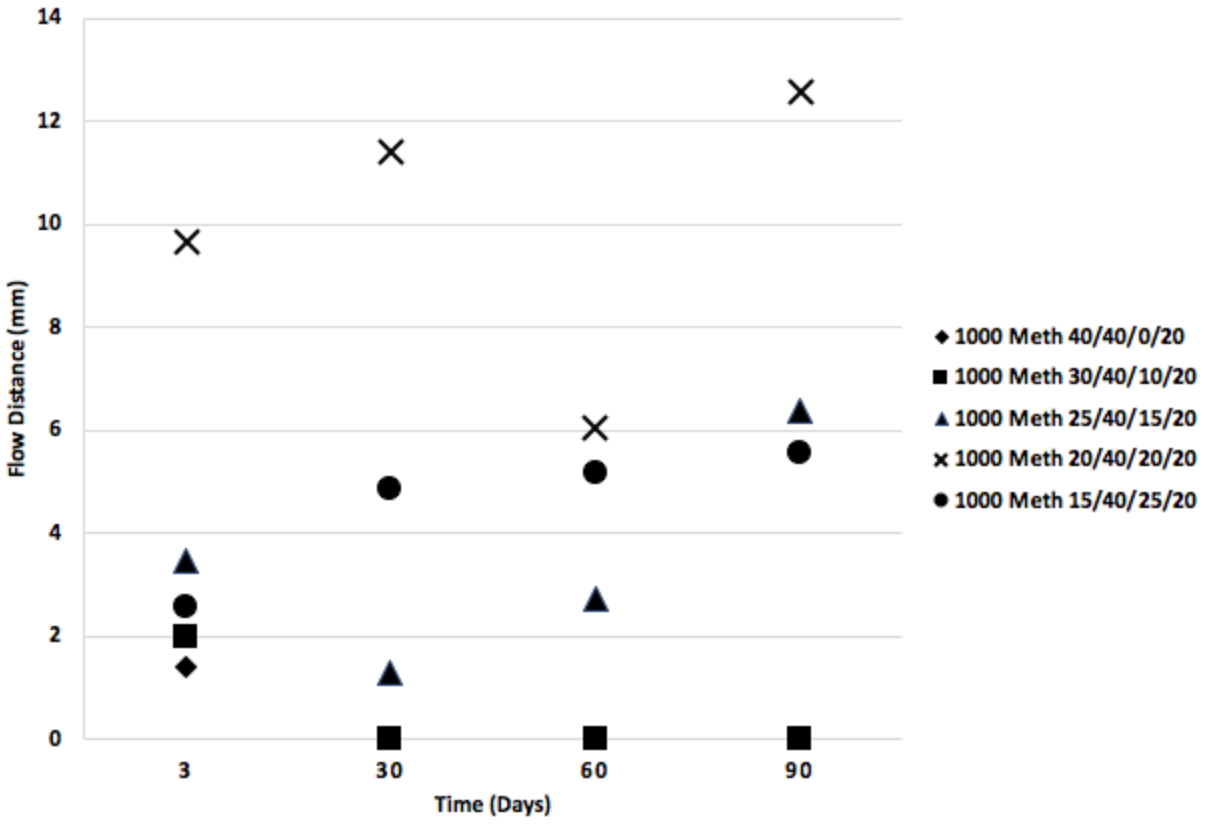

Figure 5. This graph illustrates the distance a constant mass of 1000 Meth formulation flowed in 30 seconds as a function of time after the formulation was prepared. The 5 different formulation identities differ by continuous phase ratio of UDMA and LVM presented as UDMA/TEGMA/LVM/LSM. Each formulation was loaded with 45 w/w% glass, 2 w/w% fumed silica, and 7 w/w% microcapsules.

Figure 5 differs from figures 1, 2, and 4 by changing the glass loading to 45 w/w%. The 5 formulations all contain 1000 Meth as the low stress monomer. Each formulation contains 2 w/w% fumed silica and 7 w/w% microcapsules. The formulation identities differ by continuous phase ratio of UDMA and LVM. The largest initial flow was recorded to be 9.7 mm by 20/40/20/20. The smallest initial flow distance was 1.4 mm by 40/40/0/20. The largest overall flow during the 90-day period was recorded to be 12.6 mm on day 90 by 40/40/0/20.

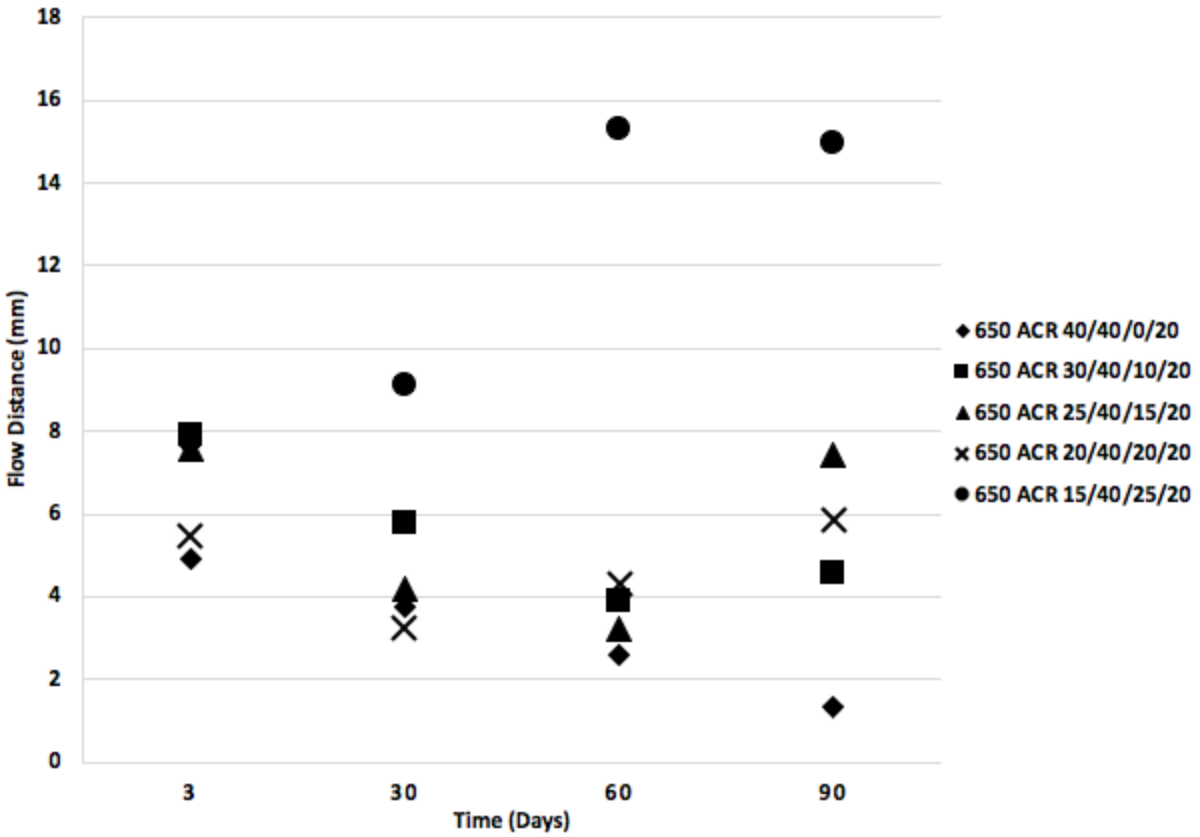

Figure 6. This graph illustrates the distance a constant mass of 650 ACR formulation flowed in 30 seconds as a function of time after the formulation was prepared. The 5 different formulation identities differ by continuous phase ratio of UDMA and LVM presented as UDMA/TEGMA/LVM/LSM. Each formulation was loaded with 45 w/w% glass, 2 w/w% fumed silica, and 7 w/w% microcapsules.

Figure 6 differs from figure 5 by changing the low stress monomer to 650 ACR. Each formulation was loaded with 45 w/w% glass, 2 w/w% fumed silica, and contained 7 w/w% microcapsules. Each formulation differed by continuous phase ratio of UDMA and LVM. The largest initial flow distance was recorded to be 7.9 mm by 30/40/10/20. The smallest initial flow distance was recorded to be 4.9 mm by 40/40/0/20. The largest overall flow distance was recorded to be 15.3 mm on day 60 by 15/40/25/20. The smallest flow distance was 1.3 mm by 40/40/0/20 on day 90.

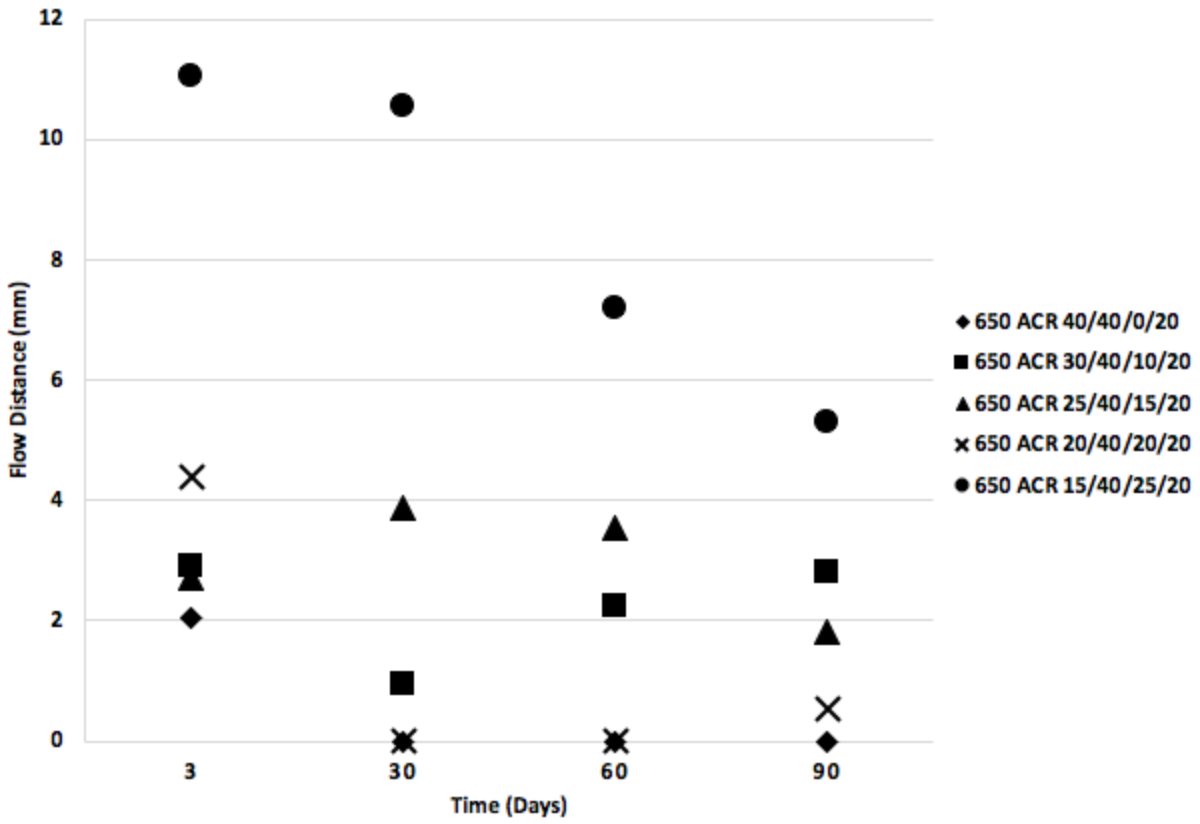

Figure 7. This graph illustrates the distance a constant mass of 650 ACR formulation flowed in 30 seconds as a function of time after the formulation was prepared. The 5 different formulation identities differ by continuous phase ratio of UDMA and LVM presented as UDMA/TEGMA/LVM/LSM. Each formulation was loaded with 50 w/w% glass, 2 w/w% fumed silica, and 7 w/w% microcapsules.

Figure 7 differs from figure 4 by changing the low stress monomer to 650 ACR. Each formulation contains 50 w/w% glass loading, 2 w/w% fumed silica loading, and 7 w/w% microcapsules. The different formulation identities differ by continuous phase ratio of UDMA and LVM. The largest initial and overall flow distance was recorded to be 11.1 mm by 15/40/25/20. The smallest initial flow distance was 2.1 by 40/40/0/20. The formulation 40/40/0/20 stops moving by day 30.

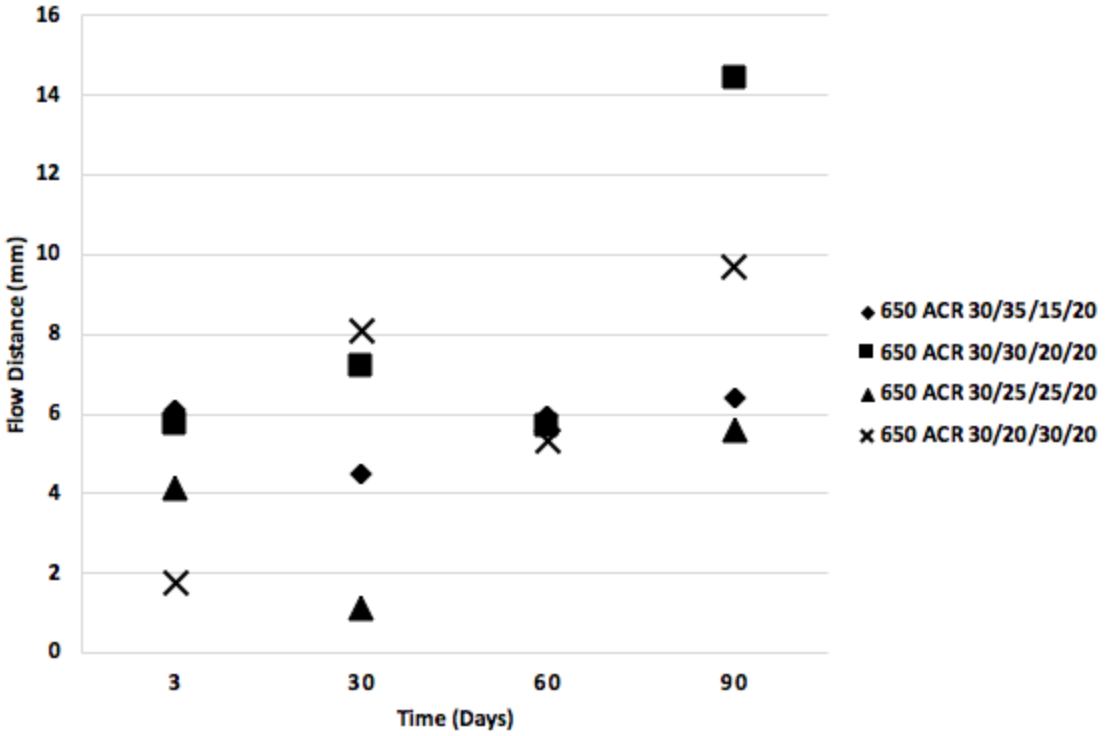

Figure 8. This graph illustrates the distance a constant mass of 650 ACR formulation flowed in 30 seconds as a function of time after the formulation was prepared. The 5 different formulation identities differ by continuous phase ratio of TEGMA and LVM presented as UDMA/TEGMA/LVM/LSM. Each formulation was loaded with 45 w/w% glass, 2 w/w% fumed silica, and 7 w/w% microcapsules.

Figure 8 differs from figure 3 by changing the glass loading to 45 w/w% and the low stress monomer to 650 ACR. Each formulation was loaded with 2 w/w% fumed silica and contained 7 w/w% microcapsules. The different formulation identities differed by continuous phase ratio of TEGMA and LVM. The largest initial flow distance was recorded to be 6.1 mm by 30/35/15/20. The smallest initial flow distance is 1.7 mm by 30/20/30/20. The largest overall flow distance was recorded to be 14.4 mm by 30/30/20/20 on day 90. The smallest overall flow distance was recorded on day 30 by 30/25/25/20 at 1.1 mm.

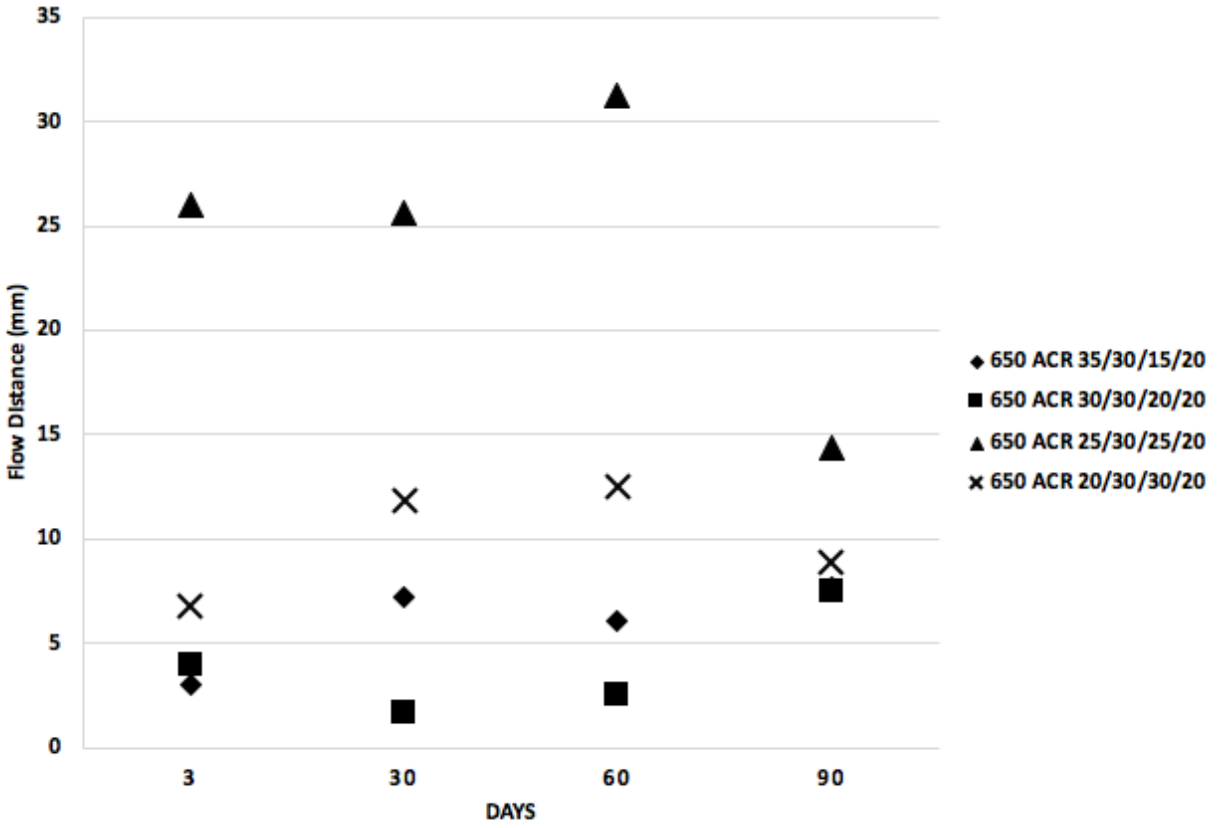

Figure 9. This graph illustrates the distance a constant mass of 650 ACR formulation flowed in 30 seconds as a function of time after the formulation was prepared. The 5 different formulation identities differ by continuous phase ratio of UDMA and LVM presented as UDMA/TEGMA/LVM/LSM. Each formulation was loaded with 38 w/w% glass, 2 w/w% fumed silica, and 7 w/w% microcapsules.

Figure 9 contained the low stress monomer 650 ACR with a glass loading of 38 w/w% and a fumed silica loading of 2 w/w%. It also contained 7 w/w% microcapsules. The different formulations within the set differed by continuous phase ratio of UDMA and LVM. The largest initial flow was recorded to be 26.0 mm by 25/30/25/20. The smallest initial flow distance was 3.0 mm by 35/30/15/20. The largest overall flow distance over the 90-day period was 31.3 mm on day 60 by 25/30/25/20.

3.2 Fumed Silica

The effect of a constant continuous phase ratio and low stress monomer of 650 ACR with varying loads of fumed silica on flow distance as a function of time was determined. Figure 10 reports the flow of various formulations over a 90-day period.

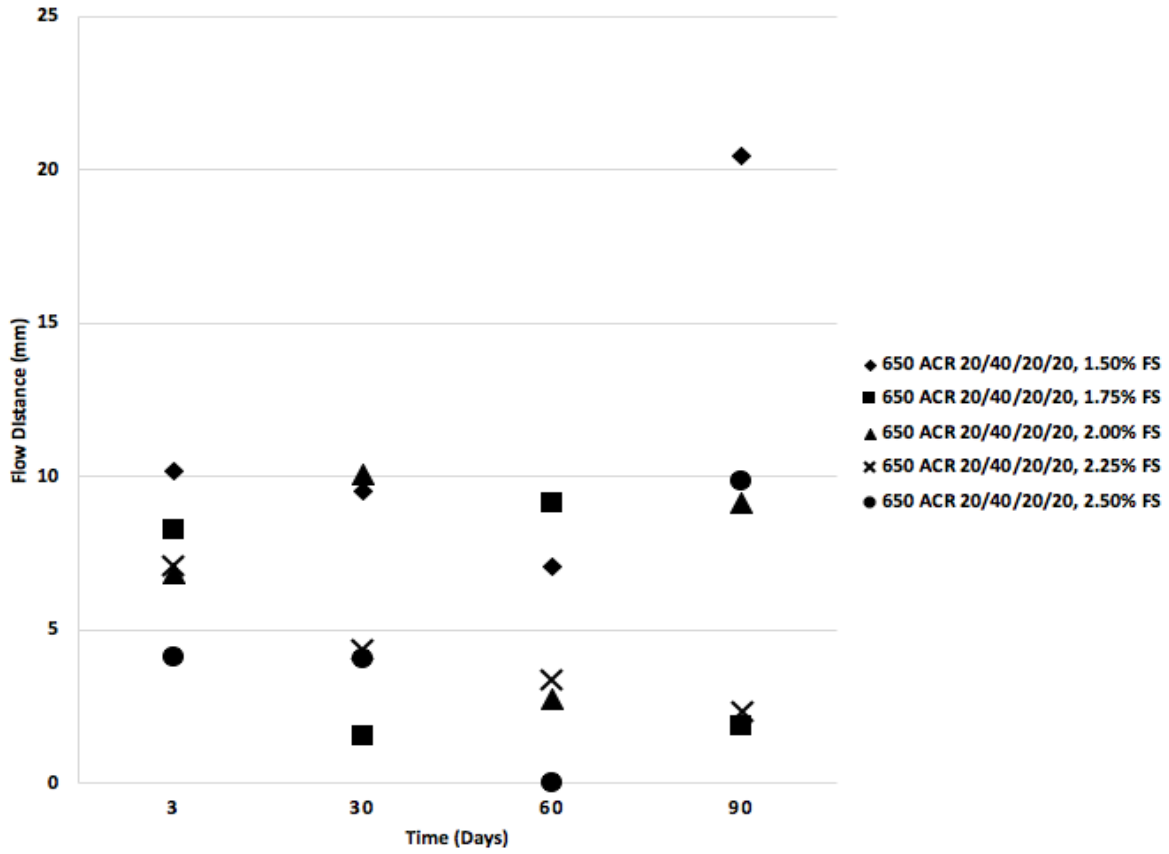

Figure 10. This graph illustrates the distance a constant mass of 650 ACR formulation flowed in 30 seconds as a function of time after the formulation was prepared. The 5 formulations each contain a constant UDMA/TEGMA/LVM/LSM ratio of 20/40/20/20. Each formulation was loaded with 38 w/w% glass, 1.50, 1.75, 2.00, 2.25, or 2.50 w/w% fumed silica, and 7 w/w% microcapsules.

Figure 10 contains 5 formulations with a constant 650 ACR low stress monomer, UDMA, TEGMA, LVM continuous phase ratio, 38 w/w% glass loading, and 7 w/w% microcapsules. Each formulation was a constant UDMA/TEGMA/LVM/LSM ratio of 20/40/20/20. The formulation set was loaded with either 1.50, 1.75, 2.00, 2.25, or 2.50 w/w% fumed silica. The largest initial flow

was recorded to be 10.2 mm by 1.50 w/w% fumed silica. The smallest initial flow was 4.1 mm by 2.50 w/w% fumed silica. The largest overall flow distance recorded was 20.5 mm on day 90 by 1.50% fumed silica.

3.3 Constant Continuous Phase Ratio and Low Stress Monomer With Varying Glass Loading

The effect of a constant continuous phase ratio and low stress monomer on flow with varying amounts of glass loading as a function of time was determined. Figures 11-20 report the flow of the various formulations over a 90-day period.

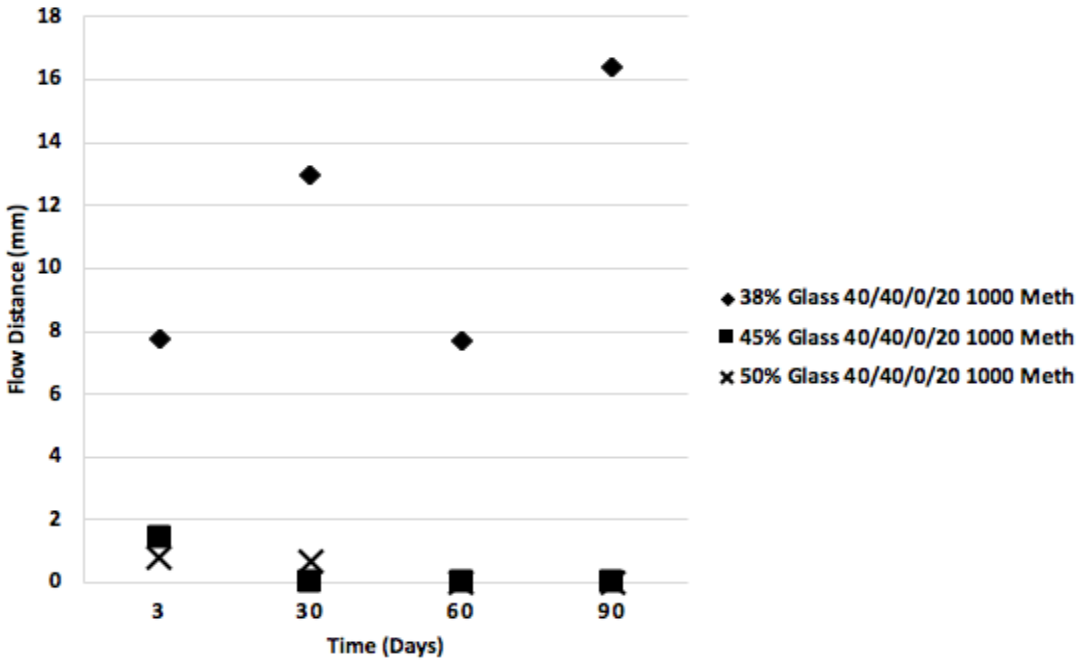

Figure 11. This graph illustrates the distance a constant mass of 1000 Meth formulation flowed in 30 seconds as a function of time after the formulation was prepared. The 3 different formulation identities differ by w/w% glass loading Each formulation was loaded with either 38, 45, or 50 w/w% glass. Each formulation contained 2 w/w% fumed silica, and 7 w/w% microcapsules. The continuous phase ratio (UDMA/TEGMA/LVM/LSM) of 40/40/0/20 was used for each formulation.

Figure 11 depicts the flow of three formulations varying only by glass loading. Each formulation consisted of a continuous phase ratio of 40/40/0/20 with either 38, 45, or 50 w/w/% glass loading. The largest initial flow was 7.7 mm by 38 w/w% glass. The smallest initial flow was 0.8 mm by 50 w/w% glass. The largest overall flow throughout the entire 90-day period was 16.4 mm on day 90 by 38 w/w% glass.

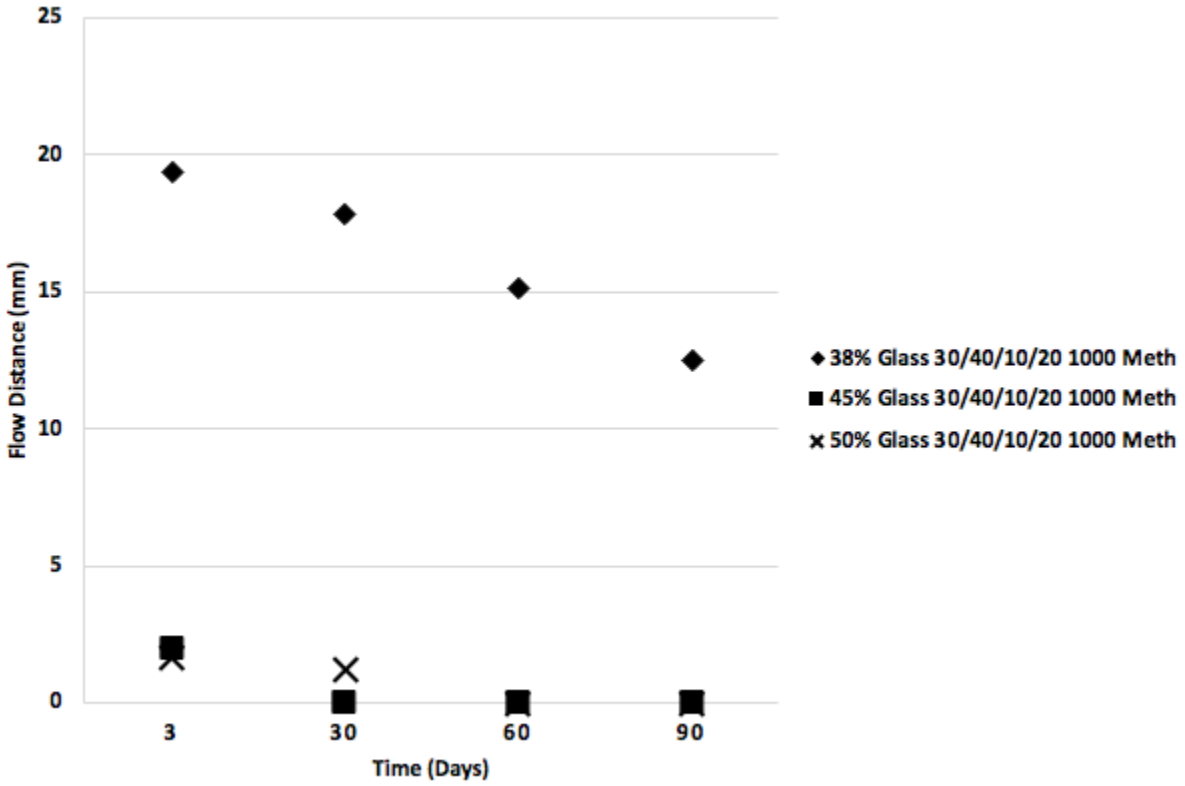

Figure 12. This graph illustrates the distance a constant mass of 1000 Meth formulation flowed in 30 seconds as a function of time after the formulation was prepared. The 3 different formulation identities differ by w/w% glass loading Each formulation was loaded with either 38, 45, or 50 w/w% glass. Each formulation contained 2 w/w% fumed silica, and 7 w/w% microcapsules. The continuous phase ratio (UDMA/TEGMA/LVM/LSM) of 30/40/10/20 was used for each formulation.

Figure 12 differs from figure 11 by changing the continuous phase ratio to 30/40/10/20 for each of the three formulations. Each formulation consisted of a continuous phase ratio of 30/40/10/20 with either 38, 45, or 50 w/w/% glass loading. 2 w/w% fumed silica and 7 w/w% microcapsules

were used for each of the formulations. The largest initial and overall flow was by 38 w/w% glass at 19.4 mm. The smallest initial flow was by 50 w/w% glass at 1.6 mm.

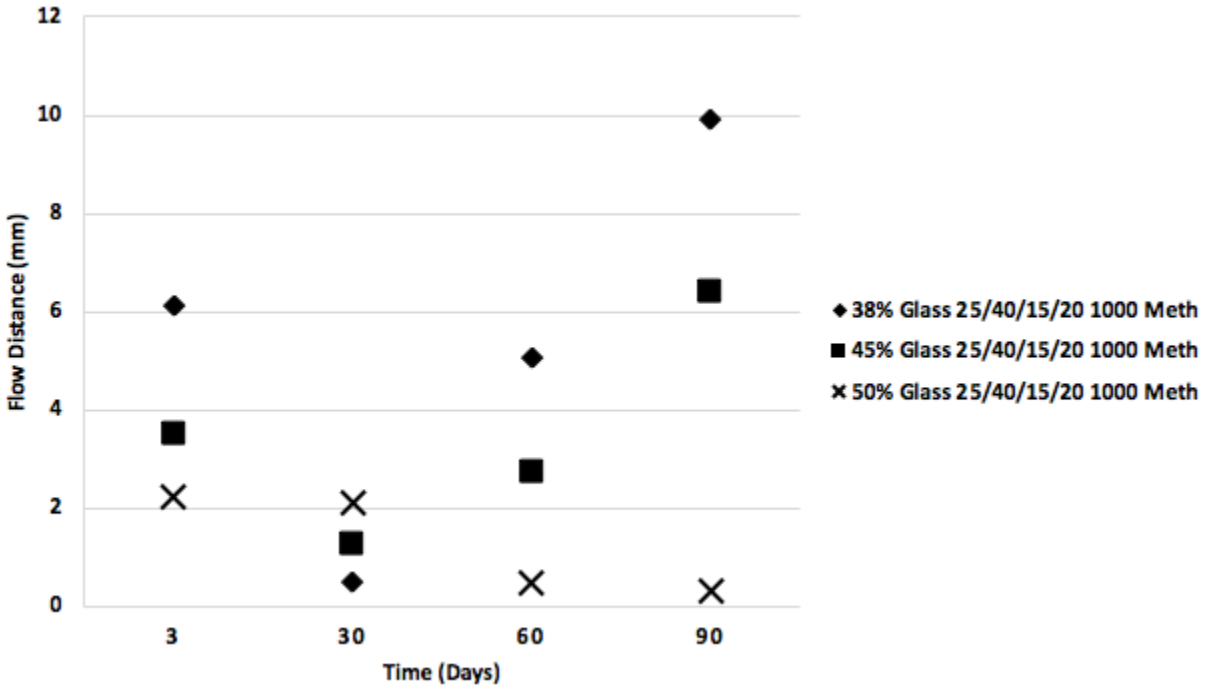

Figure 13. This graph illustrates the distance a constant mass of 1000 Meth formulation flowed in 30 seconds as a function of time after the formulation was prepared. The 3 different formulation identities differ by w/w% glass loading Each formulation was loaded with either 38, 45, or 50 w/w% glass. Each formulation contained 2 w/w% fumed silica, and 7 w/w% microcapsules. The continuous phase ratio (UDMA/TEGMA/LVM/LSM) of 25/40/15/20 was used for each formulation.

Figure 13 differs from figure 12 by changing the continuous phase ratio to 25/40/15/20. Each formulation contained 2 w/w% fumed silica and 7 w/w% microcapsules. The largest initial flow was 6.1 mm by 38 w/w% glass loading. On day 30, the 38 w/w% glass dropped to 0.5 mm before returning to 5.1 mm on day 60. The largest overall flow throughout the entire 90-day period was 9.9 mm on day 90 by the 38 w/w% glass.

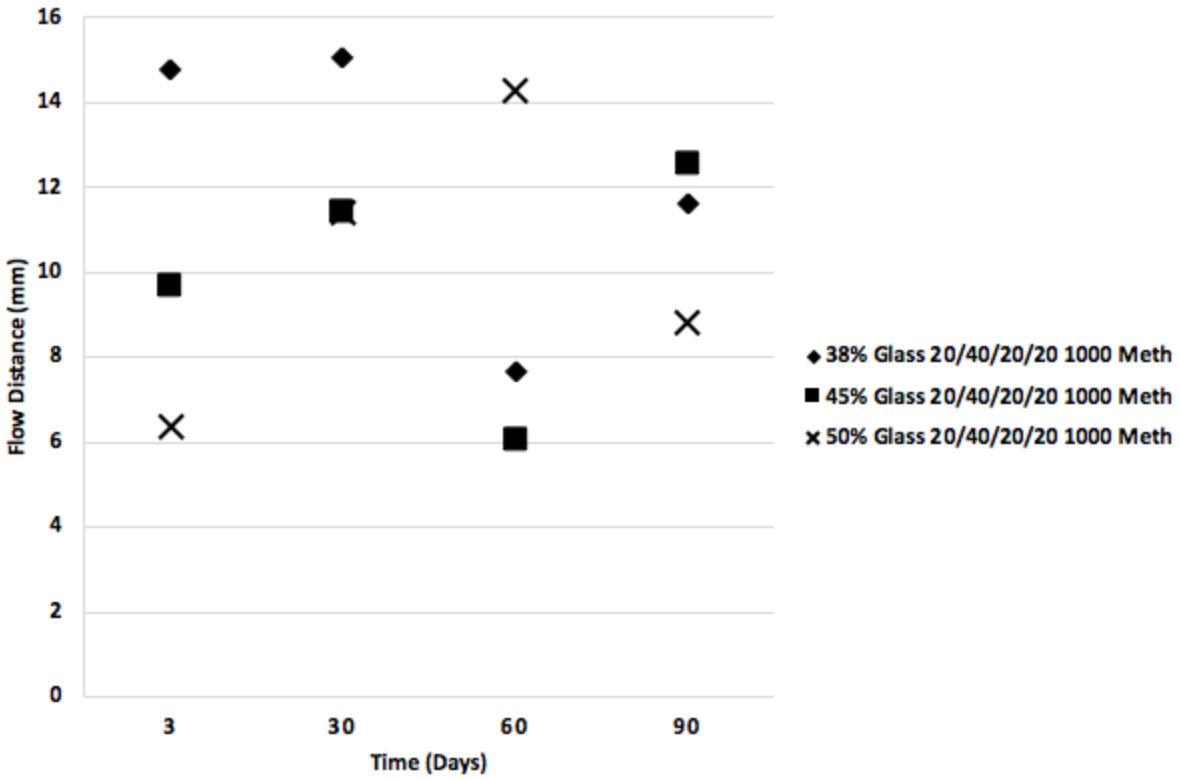

Figure 14. This graph illustrates the distance a constant mass of 1000 Meth formulation flowed in 30 seconds as a function of time after the formulation was prepared. The 3 different formulation identities differ by w/w% glass loading Each formulation was loaded with either 38, 45, or 50 w/w% glass. Each formulation contained 2 w/w% fumed silica, and 7 w/w% microcapsules. The continuous phase ratio (UDMA/TEGMA/LVM/LSM) of 20/40/20/20 was used for each formulation.

Figure 14 differs from figure 13 by changing the continuous phase ratio to 20/40/20/20 for each of the three formulations. All three of the formulations had initial flow distances around 6 - 15 mm. The largest initial flow distance was 14.8 mm by 38 w/w% glass. The smallest initial flow distance was 6.4 mm by 50 w/w% glass. The largest overall flow distance was on day 30 at 15.1 mm by 38 w/w% glass. The smallest overall flow distance was by 45 w/w% glass at 6.1 mm.

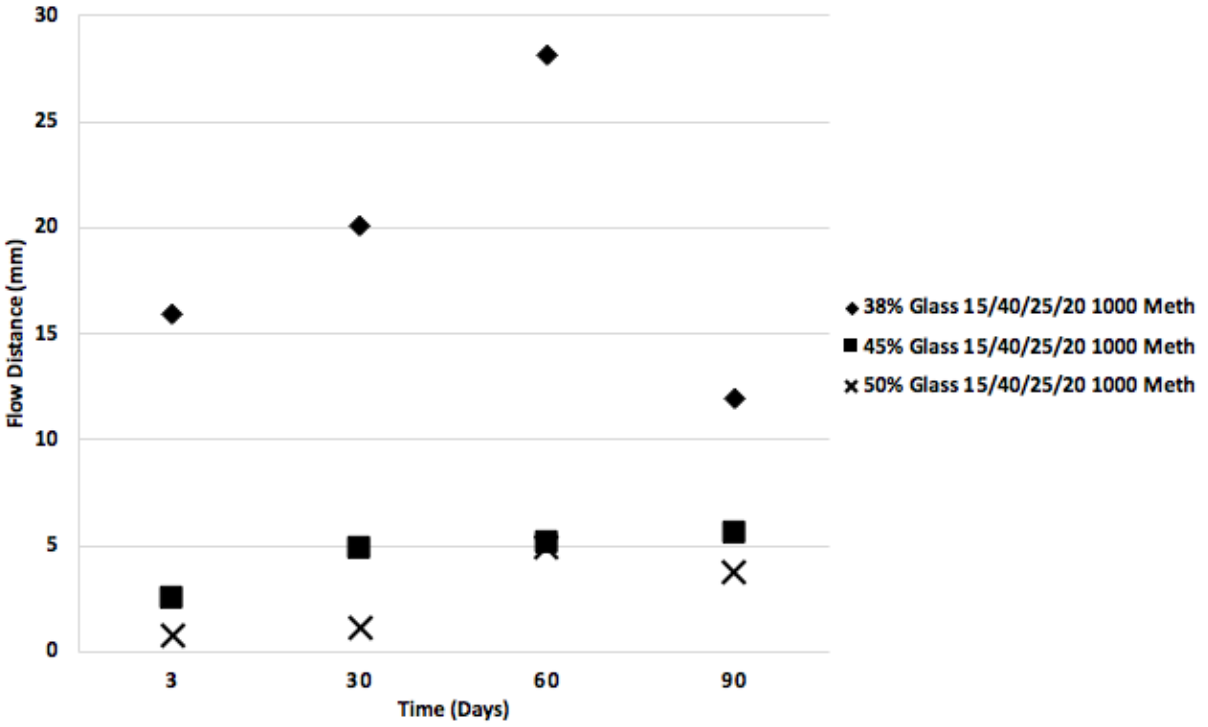

Figure 15. This graph illustrates the distance a constant mass of 1000 Meth formulation flowed in 30 seconds as a function of time after the formulation was prepared. The 3 different formulation identities differ by w/w% glass loading Each formulation was loaded with either 38, 45, or 50 w/w% glass. Each formulation contained 2 w/w% fumed silica, and 7 w/w% microcapsules. The continuous phase ratio (UDMA/TEGMA/LVM/LSM) of 15/40/25/20 was used for each formulation.

Figure 15 differs from figure 14 by changing the continuous phase ratio for each formulation to 14/40/25/20. The largest initial flow was by 38 w/w% glass at 15.9 mm. The largest overall flow throughout the entire 90-day period was 28.1 mm by 38 w/w% glass on day 60. The smallest flow distance recorded was the initial flow of the 50 w/w% glass at 0.8 mm.

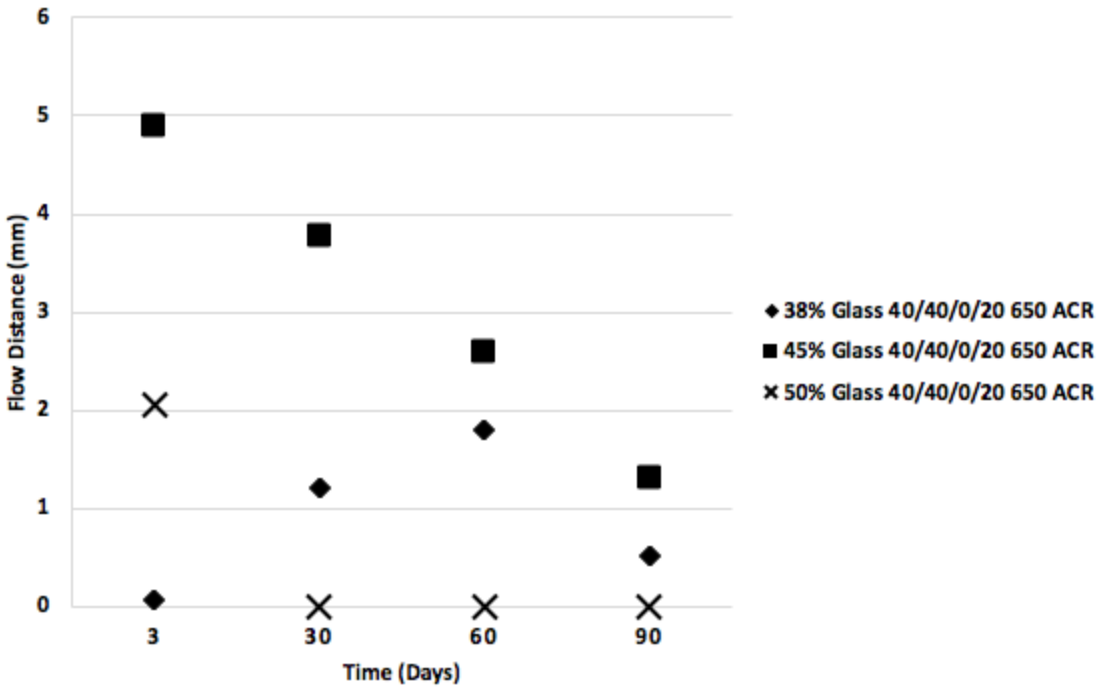

Figure 16. This graph illustrates the distance a constant mass of 650 ACR formulation flowed in 30 seconds as a function of time after the formulation was prepared. The 3 different formulation identities differ by w/w% glass loading Each formulation was loaded with either 38, 45, or 50 w/w% glass. Each formulation contained 2 w/w% fumed silica, and 7 w/w% microcapsules. The continuous phase ratio (UDMA/TEGMA/LVM/LSM) of 40/40/0/20 was used for each formulation.

Figure 16 differs from figure 15 by changing the low stress monomer to 650 ACR and the continuous phase ratio to 40/40/0/20. The largest initial flow was by 45 w/w% glass at 4.9 mm. The smallest initial flow distance was 0.1 mm by 38 w/w% glass. The 50 w/w% glass stopped flowing by day 30. All three formulations showed negative flows by day 60.

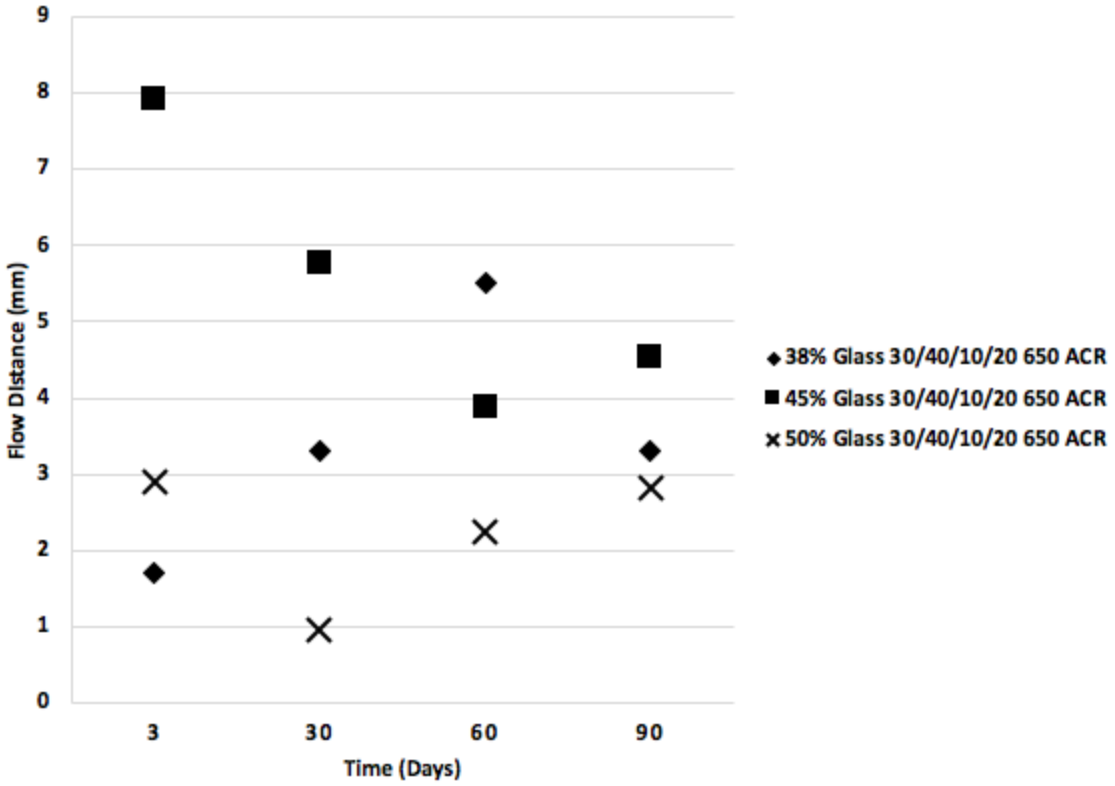

Figure 17. This graph illustrates the distance a constant mass of 650 ACR formulation flowed in 30 seconds as a function of time after the formulation was prepared. The 3 different formulation identities differ by w/w% glass loading Each formulation was loaded with either 38, 45, or 50 w/w% glass. Each formulation contained 2 w/w% fumed silica, and 7 w/w% microcapsules. The continuous phase ratio (UDMA/TEGMA/LVM/LSM) of 30/40/10/20 was used for each formulation.

Figure 17 differed from figure 16 by changing the continuous phase to 30/40/10/20. The largest initial and overall flow distance was by 45 w/w% glass 7.9 mm. The smallest initial flow distance was 1.7 mm by 38 w/w% glass. The smallest overall flow distance was recorded on day 30 by 50 w/w% glass at 1.0 mm. Every formulation was observed to converge around 3 - 4.5 mm by day 90.

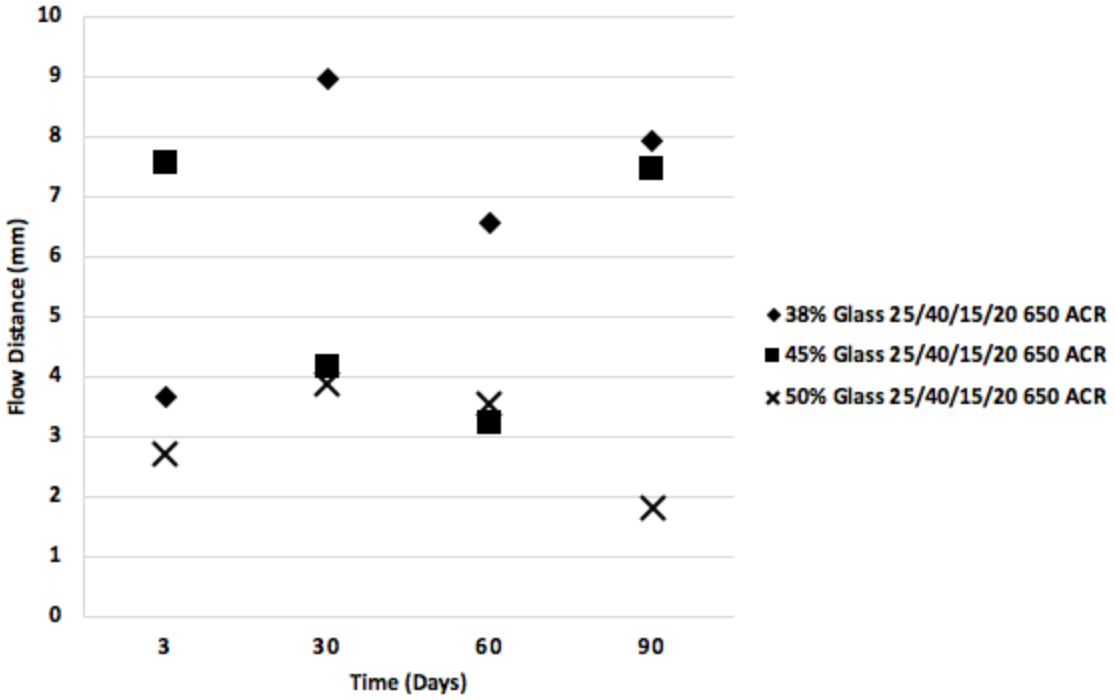

Figure 18. This graph illustrates the distance a constant mass of 650 ACR formulation flowed in 30 seconds as a function of time after the formulation was prepared. The 3 different formulation identities differ by w/w% glass loading Each formulation was loaded with either 38, 45, or 50 w/w% glass. Each formulation contained 2 w/w% fumed silica, and 7 w/w% microcapsules. The continuous phase ratio (UDMA/TEGMA/LVM/LSM) of 25/40/15/20 was used for each formulation.

Figure 18 differed from figure 17 by changing the continuous phase ratio to 25/40/15/20 for each formulation. The largest initial flow distance was by 45 w/w% glass 7.6 mm. The smallest initial flow distance was by 50 w/w% glass at 2.7 mm. The largest overall flow distance throughout the entire 90-day period was by 38 w/w% glass at 9.0 mm. The smallest overall flow distance was by 50 w/w% glass at 1.8 mm.

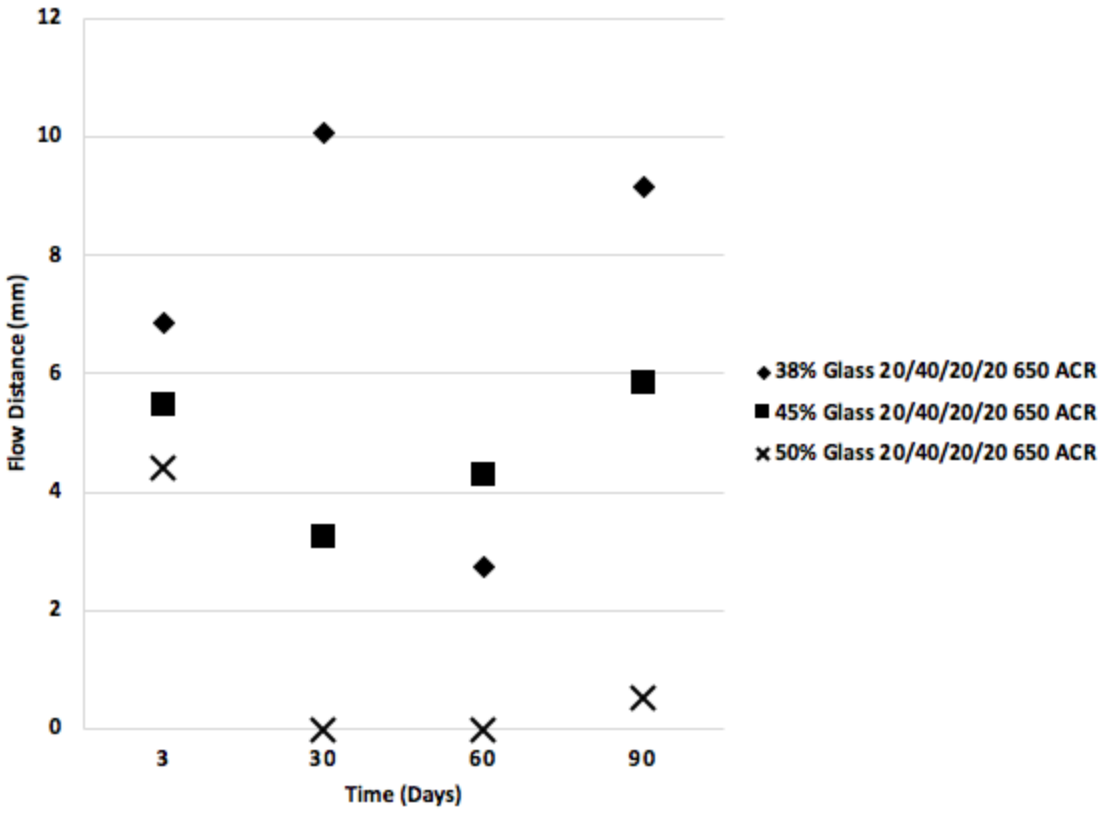

Figure 19. This graph illustrates the distance a constant mass of 650 ACR formulation flowed in 30 seconds as a function of time after the formulation was prepared. The 3 different formulation identities differ by w/w% glass loading Each formulation was loaded with either 38, 45, or 50 w/w% glass. Each formulation contained 2 w/w% fumed silica, and 7 w/w% microcapsules. The continuous phase ratio (UDMA/TEGMA/LVM/LSM) of 20/40/20/20 was used for each formulation.

Figure 19 differed from figure 18 by changing the continuous phase formulation to 20/40/20/20. The largest initial flow distance was recorded to be 6.9 mm by 38 w/w% glass. The smallest initial flow distance was by 50 w/w% glass at 4.4 mm. The 50 w/w% glass stopped flowing by day 30. However, by day 90, it seemed to start flowing again at 0.5 mm. The largest overall flow distance throughout the entire 90-day period was by 38 w/w% glass at 10.1 mm on day 30.

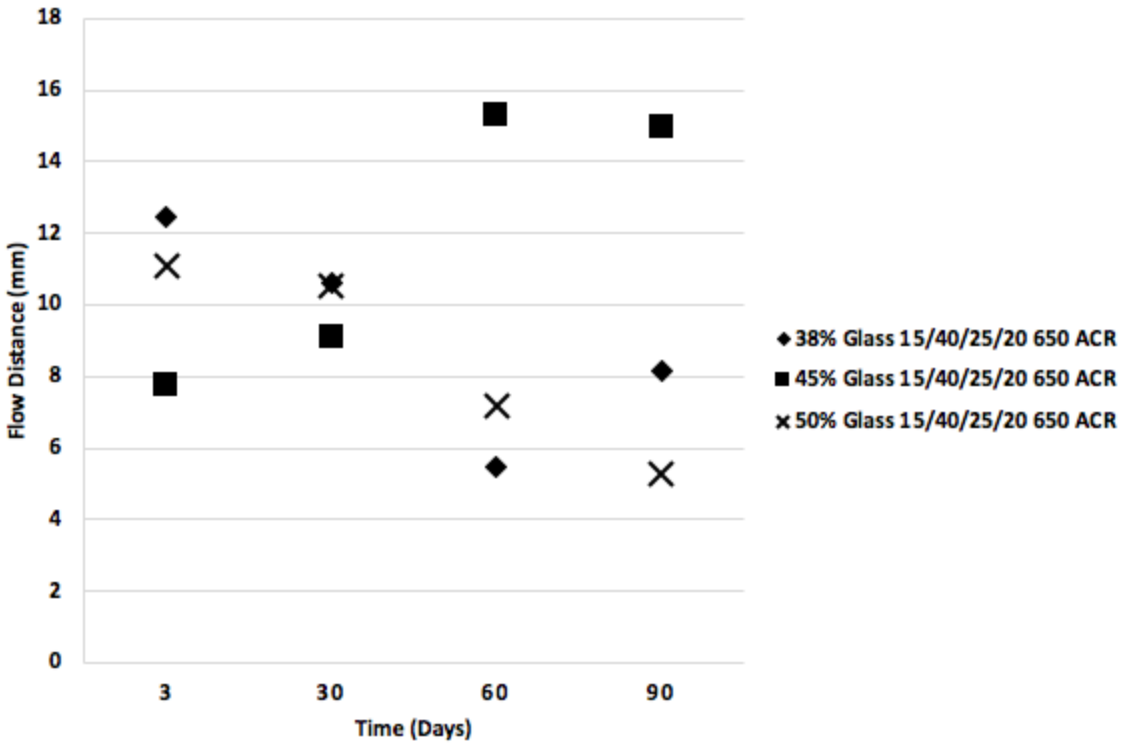

Figure 20. This graph illustrates the distance a constant mass of 650 ACR formulation flowed in 30 seconds as a function of time after the formulation was prepared. The 3 different formulation identities differ by w/w% glass loading Each formulation was loaded with either 38, 45, or 50 w/w% glass. Each formulation contained 2 w/w% fumed silica, and 7 w/w% microcapsules. The continuous phase ratio (UDMA/TEGMA/LVM/LSM) of 15/40/25/20 was used for each formulation.

Figure 20 differed from figure 19 by changing the continuous phase ratio to 15/40/25/20. The largest flow distance was recorded by 38 w/w% glass at 12.4 mm. The smallest initial flow distance was by 45 w/w% glass at 7.8 mm. The largest overall flow distance throughout the entire 90-day period was by 45 w/w% glass at 15.3 mm on day 60. The smallest overall flow distance was by 50 w/w% glass at 5.3 mm on day 90.

Chapter 4

Discussion

4.1 Discussion

The purpose of this study was to develop a new type of orthodontic sealant that includes the novel ion-releasing microcapsules. The introduction of remineralizing microcapsules requires the examination of handling characteristics and colloidal stability. Multiple formulations were created that varied by continuous phase, glass loading, and fumed silica loading to show their effect on flow and stability. Orthodontists would require predictable and consistent handling characteristics that are reflected by colloidal stability.

Post shear stress flow was measured in this study to ensure the composite formulations had specific handling characteristics. Opal® Seal™ was used as a target reference as it's a current orthodontic sealant product on the market with ion-releasing properties. As a comparison, Opal® Seal™ had a flow of approximately 6.0 mm. All of the flow measurements in this study should be observed as an approximate range due to numerous external variables. Consistent flow and measurements ranging around the target reference will be found favorable due to being colloidally stable and possessing predictable handling characteristics.

Figures 1-9 contained a constant low stress monomer (1000 Meth or 650 ACR), glass loading, and fumed silica loading with varying ratios of the continuous phase. UDMA or TEGMA were varied along with the low viscosity monomer (LVM). The continuous phase ratio was represented as UDMA/TEGMA/LVM/LSM throughout this study. The hypothesis was the increase in low viscosity monomer would result in the increase in flow without negatively affecting the colloidal stability. The null hypothesis was the addition of a low viscosity monomer will have no effect on flow and colloidal stability.

Figure 1 contained formulations with 1000 Meth as a consistent low stress monomer. Each formulation had 38 w/w% glass loading and 2 w/w% fumed silica loading. The ratio of UDMA

and LVM were varied. The formulation 25/40/15/20 is observed as not being colloidally stable due to having no flow on day 30 even though its other measurements were around the target reference. 30/40/10/20 has colloidal stability but its measurements were not close enough to be within the favorable flow range. The remaining formulations within the figure 1 set were observed to be stable except 15/40/25/20. Between days 60 and 90 it started showing signs of phase separation with a flow difference of about 17 mm between days 60 and 90. Figure 2 contained the same continuous phase ratio and glass loading except the low stress monomer was changed to 650 ACR. Figure 2 showed a relatively clearer effect of increasing ratio of LVM. As the ratio of LVM was increased, the flow generally increased. The 40/40/0/20 formulation did not contain any LVM and was observed to be the least stable and its flow was low ranging from 0 - 2 mm. Figure 3 examined the varying ratio of TEGMA and LVM with 1000 Meth as the low stress monomer. 30/30/20/20 showed colloidal instability with its large fluctuations in flow measurements. All of the other formulations in figure 3 showed stability and increased in flow as LVM was increased.

In figure 4, UDMA and LVM were varied as glass loading was increased to 50 w/w%. The increase of glass from 38 to 50 w/w% showed to have an effect on all formulation flows as compared to figure 1. LVM also has an effect on flow along with the glass loading. 20/40/20/20 and 15/40/25/20 (figure 4) were the only formulations to have any flow measurements above 2 mm while the other three formulations (40/40/0/20, 30/40/10/20, and 25/40/15/20) showed no flow by days 30 and 60. Figure 5 contains the exact same continuous phase ratios as figure 4 but lowers the glass loading to 45 w/w%. As compared to figure 4, glass loading and the addition of a LVM show to both have an effect on flow and stability. There were generally higher flow measurements and more stable formulations in figure 5 as compared to figure 4. In figure 5, both 40/40/0/20 and 30/40/10/20 stop flowing by day 30. Even while containing a higher ratio of LVM, 15/40/25/20

consistently showed a lower flow than 20/40/20/20. Figure 6 changes the low stress monomer to 650 ACR from 1000 Meth as in figure 5 and keeps the same glass loading at 45%. The 40/40/0/20 formulation is in a downward trend toward no flow by day 90. As expected, the 15/40/25/20 formulation contained the most LVM and had the highest flow with stable flow measurements. The remaining formulations all showed colloidal stability and being within the target reference. Figure 7 contained the same 650 ACR low stress monomer as figure 6 and increased the glass loading to 50 w/w%. The 40/40/0/20 formulation stopped flowing by day 30. This could be explained by the higher glass loading and containing no LVM. Unexpectedly, the formulation 20/40/20/20 stopped flowing by day 30 and flowed just 0.5 mm on day 90. The formulation ratios around it both showed flow.

Figure 8 contained 45 w/w% glass loading with 650 ACR in the continuous phase and varied by TEGMA and LVM. 30/35/15/20 formulation with the highest TEGMA to LVM ratio was recorded to be the most stable and closest to the target reference within the set. Figure 9 contained the same continuous phase ratios but varied UDMA and LVM and changed the glass loading to 38 w/w%. 25/30/25/20 showed the highest flow measurements and had the greatest differences in flow between the other formulations in the set. It wasn't as stable as the others due to a large decrease in flow by day 90 due to phase separation.

Figure 10 contained a constant low stress monomer (650 ACR) and continuous phase ratio of 20/40/20/20 portrayed as UDMA/TEGMA/LVM/LSM. Each formulation was loaded with 38 w/w% glass, 1.50, 1.75, 2.00, 2.25, or 2.50 w/w% fumed silica. Within the formulations, the glass particles tend to naturally agglomerate and sediment over time with the glass filler phase and monomer continuous phase separating. This creates fluctuations and inconsistent flow measurements. Fumed silica acts to stabilize the formulas through electrostatic repulsion. The

hypothesis was the increase in fumed silica would decrease flow and increase colloidal stability. The null hypothesis was the increase in fumed silica would have no effect on flow and colloidal stability on the formulations.

In figure 10, the formulation with the smallest amount of fumed silica loading at 1.50 w/w% had the largest average flow measurements. On day 90, there was a large fluctuation of about 13 mm showing signs of phase separation and colloidal instability. An increase to 1.75 w/w% fumed silica still shows small fluctuations in the flow. 2.00 w/w% fumed silica loading was observed to be the most stable in the set. 2.25 w/w% fumed silica was stable but had a negative trend coming close to 0 mm. The largest amount of fumed silica loading at 2.50 w/w% stopped flowing by day 60.

From the trend found in figure 10, the null hypothesis is supported. The increase in fumed silica did decrease flow and increase stability only up 2.00 w/w%. Formulations below would experience colloidal instability through phase separation by lacking a sufficient amount of fumed silica. Formulas above the 2.00 w/w% would experience lower flow and/or stop flowing.

Figures 11-20 contained a constant continuous phase ratio and low stress monomer with varying glass loading. Three different formulation identities contained either 38, 45, or 50 w/w% glass loading. Higher glass loading is preferred for the increase in strength and longevity of the composite.

Figure 11 contained the continuous phase ratio of 40/40/0/20 and 1000 Meth as the LSM for each formulation. The 38 w/w% glass formula showed flow throughout the 90-day period with fluctuations. 45 and 50 w/w% glass initially showed low flow and both stopped flowing by day 30. Figure 12 contained continuous phase ratios of 30/40/10/20, increasing the LVM. Again, only the 38 w/w% glass showed consistent and higher flow. Figure 13 contains continuous phase ratios

of 25/40/15/20. The decrease in UDMA and increase in LVM can now be clearly seen. All three formulations have higher average flow measurements as compared to figures 11 and 12. The 38 w/w% glass had even larger fluctuations and the highest flow. As glass w/w% increased, the flow distance decreased, with 50 w/w% glass almost showing no flow by day 90. Figure 14 contained the continuous phase ratios of 20/40/20/20. All three formulations showed colloidal stability with flows between 6-15 mm. Again, as expected, the higher the w/w% of glass loading the higher the average flow. Figure 15 contained the continuous phase ratios of 15/40/25/20. Only the formulas with 45 and 50 w/w% glass loading showed colloidal stability. The 38 w/w% glass showed signs of phase separation by day 90.

Figure 16 contained a constant low stress monomer of 650 ACR and continuous phase ratios of 40/40/0/20. Both 45 and 50 w/w% glass loading formulas showed colloidal instability. This could be due to a high UDMA ratio and containing no LVM with a higher glass w/w%. The 38 w/w% glass formula initially starts at 5 mm and steadily declines to about 1 mm, possibly starting to show signs of progressive instability. Figure 17 increases the LVM ratio to 30/40/10/20. All three formulations show signs of stability with 45 w/w% glass having the highest average flow. Figure 18 contains the continuous phase ratios of 25/40/15/20. The higher LVM and lower UDMA ratios in figure 18, as compared to figures 16 and 17, show higher average flow rates. Figure 19 contains the continuous phase ratios of 20/40/20/20. The 50 w/w% glass formula stops flowing by day 30. The 38 w/w% glass formula shows signs of phase separation on day 60 by the large fluctuation. Only the 45 w/w% glass formula shows signs of colloidal stability. Figure 20 contains the continuous phase ratios of 15/40/25/20. As the lowest UDMA and highest LVM ratio, it has the highest flow measurements and all formulas show stability.

4.2 Conclusion

In conclusion, the data suggests glass loading and LVM had an effect on flow. Glass loading affected the average flow of formulations. The higher the glass loading, the lower the average flow measurements for all formulations within a set. This was expected as a higher glass filler within a composite decreases flow but increases strength, wear-resistance, and longevity. The LVM had an effect on both flow and stability. As LVM was increased, the flow increased for the formulations. Formulas with a higher LVM ratio were observed to be relatively more stable than the ones with a lower LVM ratio.

References

1. Wade, W. G. (2013). “The oral microbiome in health and disease.” Pharmacological research, 69(1), 137-143.

2. Selwitz, Robert H, et al. “Dental Caries.” *The Lancet*, Elsevier, 4 Jan. 2007.

3. Dubroc, Glenn C., et al. “Reduction of Caries and of Demineralization around Orthodontic Brackets: Effect of a Fluoride-Releasing Resin in the Rat Model.” *American Journal of Orthodontics and Dentofacial Orthopedics*, Mosby, 13 July 2009.

4. Saliman, Manal M. “Fluoride Release Rate from an Orthodontic Sealant and Its Clinical Implications.” *The Angle Orthodontist*, An International Journal of Orthodontics and Dentofacial Orthopedics, 2006.

5. Baroudi, Kusai, and Jean C Rodrigues. “Flowable Resin Composites: A Systematic Review and Clinical Considerations.” *Journal of Clinical and Diagnostic Research : JCDR*, JCDR Research and Publications (P) Limited, June 2015.

6. Leizer, Cary, and Martin Weinstein. “Efficacy of a Filled-Resin Sealant in Preventing Decalcification during Orthodontic Treatment.” *Ajo-Do*, American Journal of Orthodontics and Orthopedics, 2010.

7. Davidson, Michael T., et al. “Ion Permeable Microcapsules for the Release of Biologically Available Ions for Remineralization.” *Wiley Online Library*, John Wiley & Sons, Ltd, 30 Dec. 2011.

8. Fu, Jing, et al. “Characterization of a Low Shrinkage Dental Composite Containing Bis Methylene Spiro Orthocarbonate Expanding Monomer.” *International Journal of Molecular Sciences*, Molecular Diversity Preservation International (MDPI), 10 Feb. 2014.

9. Kleverlaan, Cornelis J., and Albert J. Feilzer. “Polymerization Shrinkage and Contraction Stress of Dental Resin Composites.” *Dental Materials*, Elsevier, 22 July 2005.

10. Luck, Russell M, and Rajender K Sadhir. *Expanding Monomers*. CRC Press, 1992.

11. Gonçalves, Flávia, et al. “BisGMA/TEGDMA Ratio and Filler Content Effects on Shrinkage Stress.” *Dental Materials*, Elsevier, 2 Mar. 2011.

12. Kwon, Youngchul, et al. “Effect of Layering Methods, Composite Type, and Flowable Liner on the Polymerization Shrinkage Stress of Light Cured Composites.” *Dental Materials*, Elsevier, 8 May 2012.

13. Suh, B I, et al. “The Effect of the Pulse-Delay Cure Technique on Residual Strain in Composites.” *Compendium of Continuing Education in Dentistry (Jamesburg, N.J. : 1995)*, U.S. National Library of Medicine, Feb. 1999.

14. Ferracane, Jack L. “Resin Composite-State of the Art.” *Dental Materials*, Elsevier, 18 Nov. 2010.

15. Baroudi, Kusai, and Said Mahmoud. “Improving Composite Resin Performance Through Decreasing Its Viscosity by Different Methods.” *The Open Dentistry Journal*, Bentham Open, 26 June 2015.

16. Dawes, Colin. “What Is the Critical PH and Why Does a Tooth Dissolve in Acid?” *CDA*, Can. Dent. Association, 2003.

17. Pajor, Kamil, et al. “Hydroxyapatite and Fluorapatite in Conservative Dentistry and Oral Implantology-A Review.” *Materials (Basel, Switzerland)*, MDPI, 22 Aug. 2019.

18. Magalhães, Ana Carolina, et al. “Effect of Calcium Pre-Rinse and Fluoride Dentifrice on Remineralisation of Artificially Demineralised Enamel and on the Composition of the Dental Biofilm Formed in Situ.” *Archives of Oral Biology*, Pergamon, 7 Aug. 2007.

19.Premaraj, T S, et al. “In Vitro Evaluation of Surface Properties of Pro Seal® and Opal® SealTM in Preventing White Spot Lesions.” *Orthodontics & Craniofacial Research*, U.S. National Library of Medicine, June 2017.

20. Burbank, Brant, et al. “Ion Release and in Vitro Enamel Fluoride Uptake Associated with Pit and Fissure Sealants Containing Microencapsulated Remineralizing Agents .” *American Journal of Dentistry*, 2017.

21. Usha, Carounanidy, and Sathyanarayanan R. “Dental Caries - A Complete Changeover (Part I).” *Journal of Conservative Dentistry : JCD*, Medknow Publications, Apr. 2009.